

We are IntechOpen, the world's leading publisher of Open Access books Built by scientists, for scientists

6,900

Open access books available

186,000

International authors and editors

200M

Downloads

Our authors are among the

154

Countries delivered to

TOP 1%

most cited scientists

12.2%

Contributors from top 500 universities



WEB OF SCIENCE™

Selection of our books indexed in the Book Citation Index
in Web of Science™ Core Collection (BKCI)

Interested in publishing with us?
Contact book.department@intechopen.com

Numbers displayed above are based on latest data collected.
For more information visit www.intechopen.com



Cu-Based Shape Memory Alloys: Modified Structures and Their Related Properties

Safaa Najah Saud Al-Humairi

Abstract

Cu-Al-Ni shape memory alloys (SMAs) have been developed for high-temperature applications due to their ability to return to pre-deformed shape after heating above the transformation temperature, as well as these alloys have a small hysteresis and high transformation temperature comparing with other shape memory alloys. Adding some of the alloying elements such as Ti, Mn, Be, Zr and B or changing the interior content either Al or Ni by increasing/decreasing may have a significant effect on the phase transitions and enhance the mechanical properties of these alloys. However, the martensite phase transformation is the most important factor, which can be changing the whole properties of Cu-Al-Ni SMAs, where this phase is mainly affected by the alloying elements additions. This chapter reviews the effect of alloying elements on the phase transitions and the enhancement of the mechanical properties of this alloy.

Keywords: shape memory alloys, martensitic transformation, Cu-Al-Ni, grain refinement, alloying elements

1. Introduction

Shape memory alloys (SMAs) are insightful types of materials that is designed to undertake the phase transformation of martensitic phase once the thermomechanical loads are employed, and also in a position to restore their initial form as soon as heated up above particular temperatures [1–3]. A couple of symmetries take place for the structural morphologies within this kind of the materials; high symmetry at high-temperature is known as austenite and also a low symmetry at lower temperatures known as martensite. The martensitic transformation that starts for the transformation of austenite (high temperature phase) \rightleftharpoons martensite (low temperature phase), is the principal characteristic in charge of shape memory alloys features. Furthermore, this transformation is prominent as diffusionless solid-state step of transformation which is presented by means of nucleation, accompanied by the formation route of the relative austenitic phase [4, 5]. Due to the pseudo-elasticity and shape memory effect (SME) properties, the shape memory alloys have been remarkably distinguished compared to other types of materials [6–8], in which they are completely related the incidence of martensitic phase transformation. The variant crystal structure disparities take place during the phase transformation of a cubic structure (austenite) transferred to a monoclinic structure (martensite).

These sorts of martensite forms have the ability to be organized independently in a self-accommodation approach by the mechanism of twinning throughout the inadequacy of the practiced stresses, with the consequence that virtually no shape transform can certainly be realized. The results of martensitic phase deformation are able to be detwinned into a single variant corresponded to the applied loads, and consequently a large inelastic strain happened [9, 10]. Heating the deformed alloys to a certain temperature above the austenite temperature will turn the inelastic strain to be recovered through transferring the existed martensite to austenite, this kind of feature is known as shape memory effect (SME) [9]. On the other hands, the pseudo-elasticity (PE) is caused by transferring the twinned martensitic phase into detwinned phase and obtained the shape recovery under the austenite starts temperature; in other words, the deformation of loading and unloading will be occurred in the austenite phase. This kind of structure transfer will be resulted in a large inelastic strain and a consequence of the phase reverse transformation, the initial shape will be restored upon the unloading process. Therefore, these types of materials such as Ti-based, Cu-based, and Fe-based SMAs are capable to demonstrated SME and PE [11–13]. Generally, there are two groups of martensitic transformation, thermoelastic and non-thermoelastic [14]. The thermoelastic martensitic transformations happen during the mobile interfaces between the martensite phase and parent phase. These types of interfaces are able to move during the reverse martensitic transformation as an alternative to the nucleation of the parent phase, which leads to a crystallographically reversible transformation [1]. On the other hand, the non-thermoelastic martensitic transformations are mainly found in ferrous alloys, which are related to the non-mobile interfaces of the martensitic parent phase pinned by permanent defects leading to a successful nucleation and growth. As a result of the austenite re-nucleation during the reversible martensitic transformation, these kinds of transformations are crystallographically non-reversible, in which the martensite phase is not able to return to original phase [15].

2. Shape memory characteristics

2.1 Shape memory effect property

Shape memory effect (SME) is a property of SMAs which enable thermoelastic martensitic transformation. Shape memory effect will occur with the deformation of the SMA in the martensitic phase during the loading and unloading at temperatures below M_f . After heating these deformed alloys to a temperature above A_f , the austenite phase forms, and thus, the original shape is recovered. **Figure 1** shows a typical loading path $1 \rightarrow 2 \rightarrow 3 \rightarrow 4 \rightarrow 1$, wherein the property of SME is observed [16]. The parent phase transforms into the twined martensite ($1 \rightarrow 2$) when it undergoes the cooling process. The stress induced detwinning and inelastic strains can occur when the materials are loaded ($2 \rightarrow 3$). The martensite phase is in the same state of the detwinned structure without obtaining any recovered inelastic strains even after the unloaded process ($3 \rightarrow 4$). In the final step, the materials are returned to the original shape by recovering the inelastic strains after being heated above A_f ($4 \rightarrow 1$).

A self-accommodating growth of the martensitic variants ($1 \rightarrow 2$) is being produced within the stress-free cooling of austenite phase without observing any macroscopic transformation [17–19]. The essential morphology that characterize the crystallographic of these alloys is the self-accommodating structure. For instance, of the Cu-based shape memory alloys, there are 24 variants of martensite that consist of six self-accommodated groups distributed around $\langle 011 \rangle$ poles of

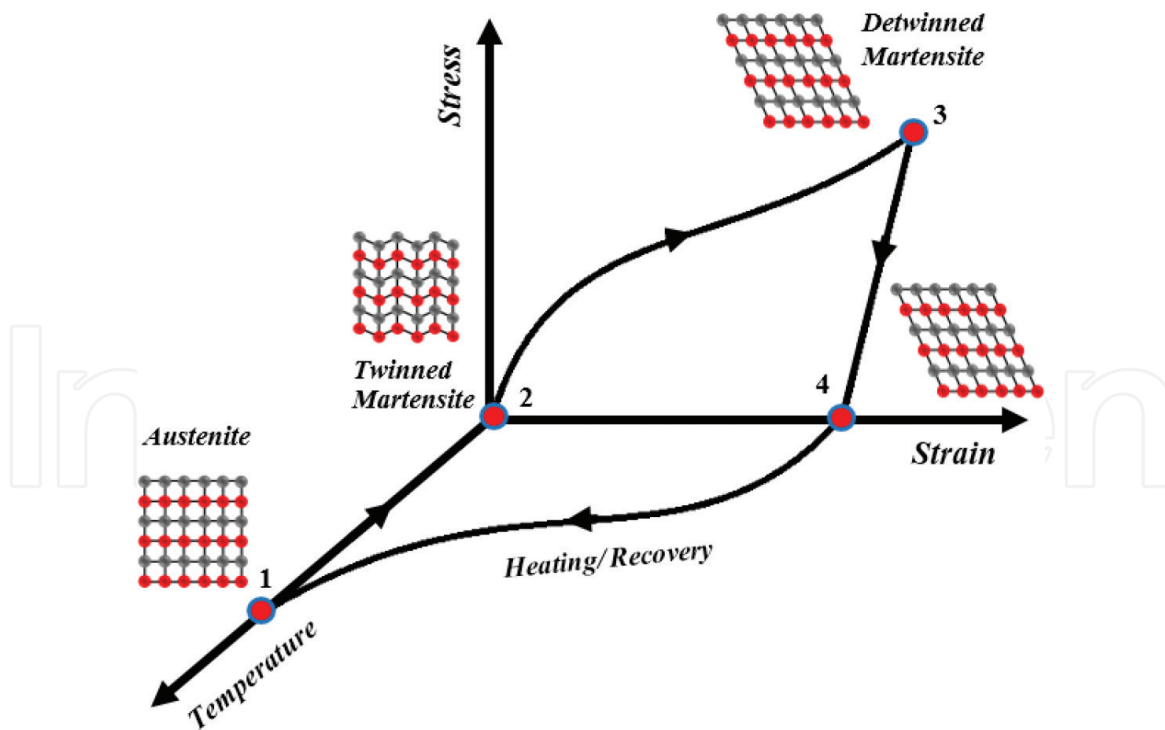


Figure 1. Schematic diagram of stress-strain-temperature for the involved crystallographic changes during the phenomena of SME [16].

austenite which exhibit an ordinary diamond morphology. During the growth process of these groups, the macroscopic transformation strain cannot be observed, except that some of the boundaries between the martensite variants and twinning interfaces display very high movements. However, the boundary interfaces together with the detwinning structure is performed at a stress level much lower than the martensite plastic yield limit, where these phenomena is known as a reorientation of variants, which dominates at temperatures lower than M_f . In the second stage (2 → 3), the loading forces are going to reorient the variants of the martensite phase, which result in producing a large value of inelastic strain, and this strain is not recovered upon unloading (3 → 4). During the last step (4 → 1), heating the deformed alloys to a certain temperature above A_f induces reverse transformation and the inelastic strain is recovered [9, 16, 20]. The martensitic phase transformation will be unstable after the austenite finish temperature (A_f) approached without requirement for any kind of external stress. It resulted in a complete recovery will be achieved, in consequence the martensite variant reorientations do occurred, there will be an additional strain with the same value of the inelastic strain but in opposite direction, and thus, the initial shape will be recovered. Saud et al. [21] was carried out the shape memory effect test using a special designed machine, as presented in **Figure 2**; whereas the test was performed at a temperature below martensite finish temperature (i.e., 100°C), the shape recovery was obtained partially, and then it was followed by a subsequent heating above the austenite finish temperature (A_f is 300°C) using an external muffle furnace, where a full recovery was achieved.

2.2 Pseudoelasticity property

The property of pseudoelasticity in the shape memory alloys is mainly related to the induced strain recovery upon unloading at temperatures above A_f . Within the general conditions, the thermomechanical loading directions of pseudoelastic are usually started in the austenitic area at zero stress, and then move toward the region

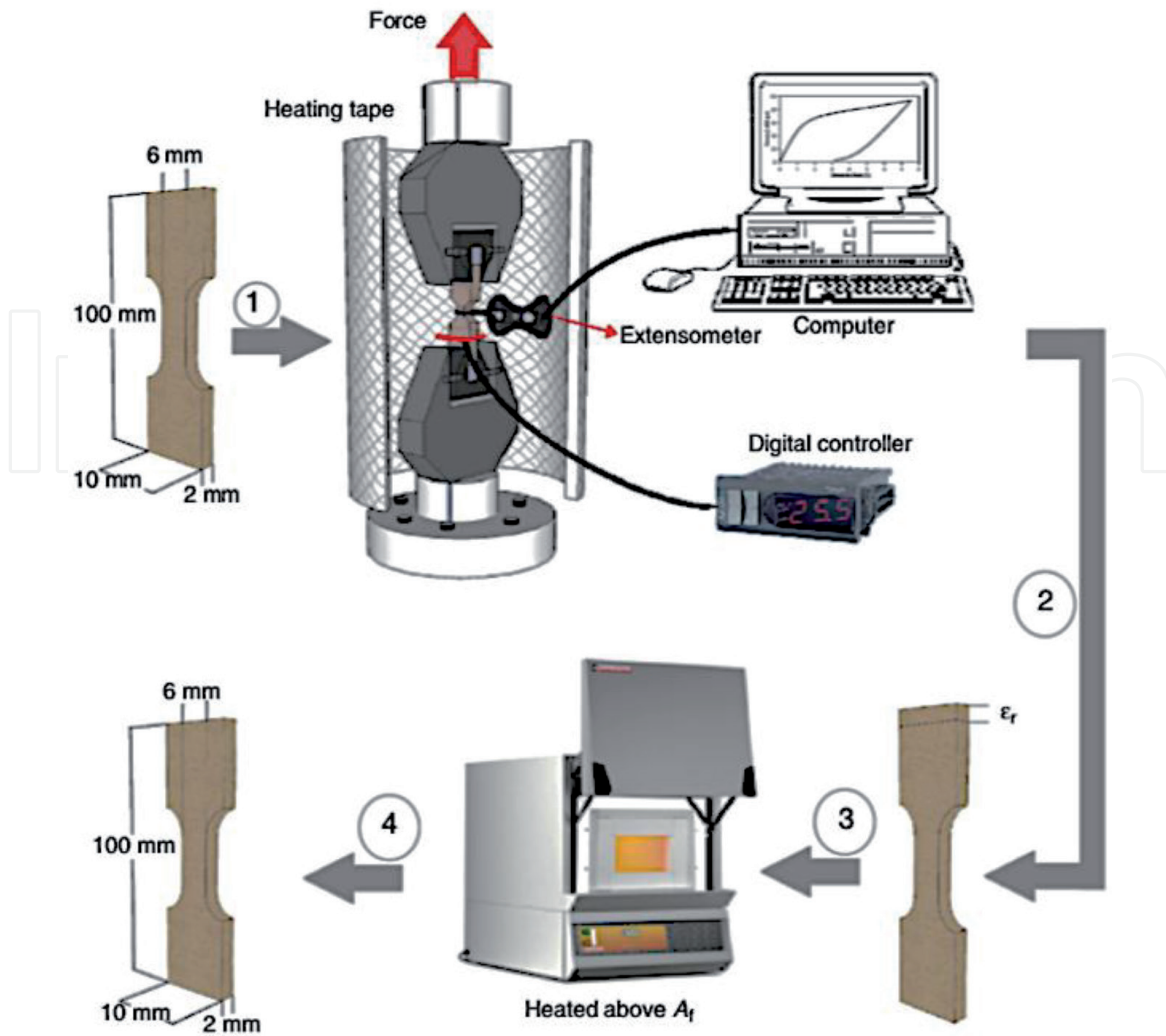


Figure 2. Shape memory effect test [21].

of detwinned martensite, followed by the unloading toward the starting point. **Figure 3** shows the loading and unloading direction that started from point *a*, and moved to *b* → *c* → *d* → *e*, then returned back to point *a*. Other examples are the isothermal and isobaric loading paths shown schematically in **Figure 3**.

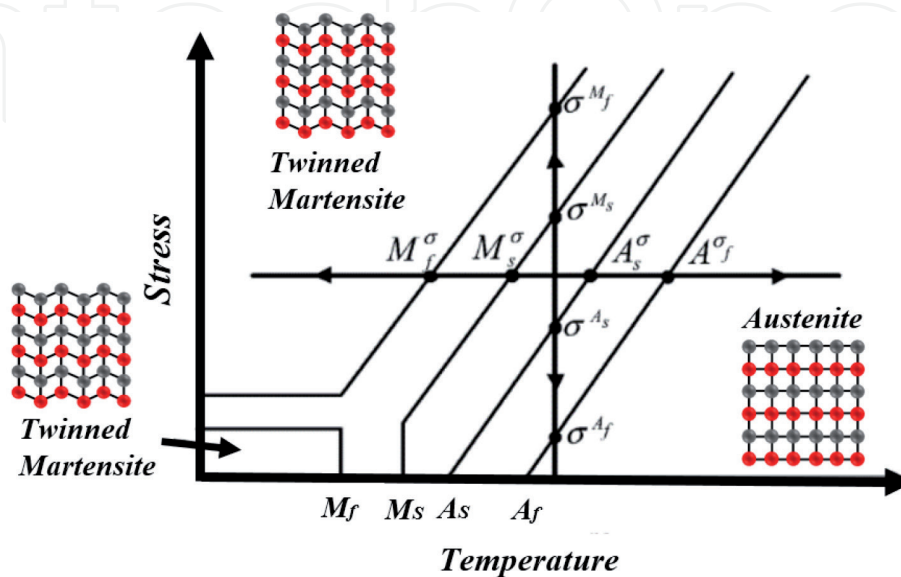


Figure 3. The two loading paths discussed for pseudoelasticity in single crystal SMA [16].

3. Cu-based SMAs

There are two main types of Cu-based SMAs; binary alloys of Cu-Al and Cu-Zn, in which both systems performed their shape memory features in the domain of β -phase, moreover, the third element addition to the binary and/or ternary is aimed to modify and control the transformation temperatures in comprehensive range in meet the application requirements, i.e., $T \approx 100\text{--}370^\circ\text{C}$. From this point of view, it was proven that the transformation temperatures are highly sensitive to the composition of alloys. Accuracy of 10^{-3} to 10^{-4} at.% is typically essential to obtain reproducibility more desirable than 5°C . Copper-based alloys commonly display considerably less hysteresis as compared to NiTi. Cu-Zn-Al alloy is not difficult to produce and is quite inexpensive. It decomposes into the equilibrium phases whenever overheated, therefore leading to a stabilization of the martensite. The properties of Cu-Al-Ni and Cu-Zn-Al SMAs are listed in **Table 1**. The availability of additives, including Co, Zr, B or Ti, is vital to provide grains from 50 to 100 nm in size. Add-on of boron is also used to enhance the ductility of the material. Cu-Al-Ni is substantially less vulnerable to stabilize as well as aging phenomena. This alloy performs with less hysteresis than NiTi and turns brittle as Ni increases much beyond 4 at.% [22]. It is also prevalent for Ni to be retained at a constant 4 at.% and this alloy is composed of $\text{Cu}_{96-x}\text{Al}_x\text{Ni}_4$ [23, 24]. In general, increasing the Al amount can lead to increase the stability of martensite. The purpose of the Al addition is to reduce the transformation temperatures. This variety is nearly entirely linear, ranging from $M_f = 203$ K and $A_f = 250$ K for a 14.4 at.% Al to $M_f = 308$ K and $A_f = 348$ K for a 13.6 at.% Al [22]. However, as the temperatures tend to be operated over a wide range; the sensible higher limit for transformation is 473 K. Above this temperature there is certainly an immediate degradation in the transformation as a result of aging effects. The typical Cu-based SMAs are able to exhibit a pseudoelastic strain of about of 4–6%. With the martensite to martensite transformation, very high pseudoelastic strain levels are displayed. A single crystal of the $\text{Cu}_{81.8}\text{Al}_{14}\text{Ni}_{4.2}$ SMA can exhibit approximately 18% of the pseudoelastic strain associated with 100% of the shape recovery [25]. Cu-Zn alloy with the addition of the third element of Sn with a weight percentage of 34.7% has exhibited very low transformation temperatures, around M_f of 208 K and an A_f of 235 K [26]. As well this addition has exhibited a transformation strain (ϵ^t) with applied strain of 2.5% along with a pseudoelastic strain of around 8% by obtaining a full strain recovery [26]. In recent years, a minor amount (about 0.6 wt.%) of beryllium was added as a third element to the binary alloy of Cu-Al, and it was found that this addition led to reduce the transformation temperatures from 200 to 150°C with very good thermal stability.

Cu-based SMAs consist of different types of alloys, but the most frequently used alloys are Cu-Zn-Al and Cu-Al-Ni due to their inexpensive production cost and high resistance to the degradation of functional properties that occurred during the aging processes. There are many features that characterized the Cu-Al-Ni SMA rather than other shape memory alloys, such as considerably cheaper than Ni-Ti alloys and high transformation temperatures.

3.1 Phase diagram of Cu-Al-Ni SMAs

Figure 4 displayed the cross section of the ternary alloys of Cu-Al-at 3 wt.% of nickel. The alloy may possibly demonstrate shape memory characteristics as long as the martensitic transformation materialized. With the intention to ascertain under-cooling, in which it vital to enforce the martensitic transformation, with a long of fully consideration that the heat treatment can never be prevented. It comes with annealing in the temperature variety of stable β phase to ensuing water quenching and resulted in the formation of β phase.

Group	No.	Alloy composition	Transformation temperature (°C)	Hysteresis (°C)	Tensile strain (%)	Strain recovery (%)	Remarks/features
Cu-based shape memory alloys	1.	Cu-Al-Ni	100–400	21.5	3–5	60–90	<ul style="list-style-type: none"> • Low cost • Reasonable shape memory • Good pseudoelastic behavior • Brittle in tension • Stable phase precipitation near 200°C • Reordering causes shift in transformation temperature in quenched specimen
	2.	Cu-Zn-Al	120	15–25	4	70–85	<ul style="list-style-type: none"> • High thermal conductivity • Reasonable recoverable shape memory strain • Inexpensive • Brittle alloys
	3.	Cu-Al-Be	150–200	20–25	3–5	80–90	<ul style="list-style-type: none"> • Reasonable recoverable shape memory strain • High transformation temperatures • High corrosion resistance
	4.	Cu-Al-Ni-Mn	230–280	15–20	3–4	90–100	<ul style="list-style-type: none"> • High shape memory behavior • Reasonable materials cost • High transformation temperatures • Good corrosion resistance
	5.	Cu-Al-Ni-Ti	120–260	12–20	2.5–4	90–100	<ul style="list-style-type: none"> • High shape memory behavior • Reasonable materials cost • High transformation temperatures • High corrosion resistance
	6.	Cu-Al-Ni-Fe	210–250	12–15	9	40	<ul style="list-style-type: none"> • Low shape memory behavior • High ductile material • Reasonable materials cost • High transformation temperatures • High corrosion resistance

Table 1.
Properties of copper-based shape memory alloys [27].

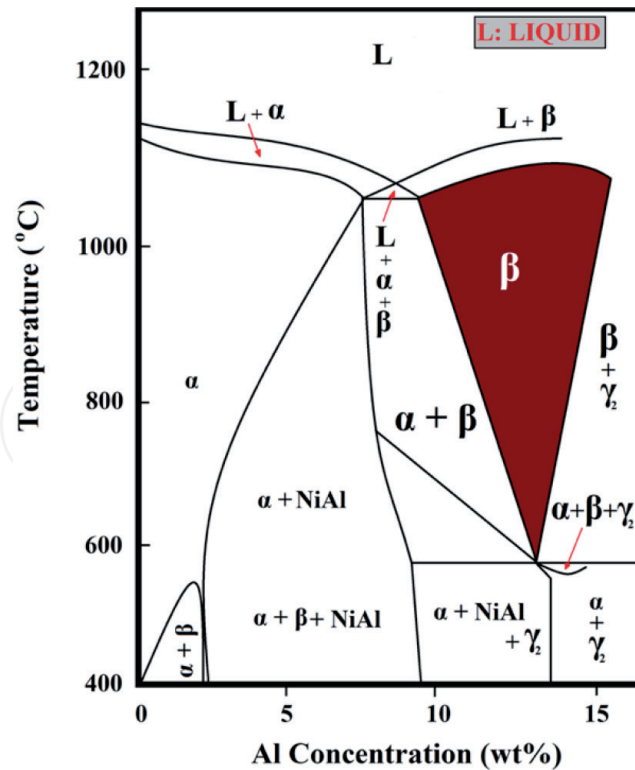


Figure 4.
 Cross-section diagram of the ternary alloy of Cu-Al-3 wt.% Ni [28].

The shape memory characteristics of Cu-Al-Ni SMA are mainly dependent on the properties of the body centered cubic β phase for the binary alloys of Cu-Al [29]. During the cooling of β phase from 565°C, this phase undergoes the eutectoid decomposition of $\beta \rightarrow \alpha + \gamma_2$. However, the high cooling rates are able to prevent this phase from eutectoid decomposition and enable the martensitic transformation. When the Cu-Al-Ni SMA possess an Al content of more than 11 wt.%, the structure of body center cubic transforms to a DO₃-type superlattice by transferring the β to order β_1 phase prior to martensitic transformation. In this case, the martensite “inherits” the ordered structure. At Al content between 11 and 13 wt.%, β'_1 martensite, having a monoclinic 18R₁ structure prevails. At Al content over 13 wt.%, orthorhombic 2H-type γ'_1 martensite prevails. Which of them will appear depends on the temperature and the stress condition. In addition to these two, other types of martensite can also form (see in **Figure 5**).

The characteristic temperatures of Cu-Al-Ni alloys can lie between –200 and 200°C dependent on content of Al and Ni; the content of Al has great influence, giving them the permittivity to be used for high temperature applications. The transformation temperatures of Ni-Ti alloys can be adjusted in the range between –200 and 120°C [31]. The A_f temperature of Fe-based SMAs can increase to approximately 300°C; but at the same time, the M_s remains at room temperature or even below. The M_s temperature can be estimated using the following empirical equation [32]:

$$M_s(^{\circ}\text{C}) = 2020 - 134 \times (\text{wt.\%Al}) - 45 \times (\text{wt.\%Ni}) \quad (1)$$

The addition of Al wt.% to the Cu-based shape memory alloys can lead to reduce the transformation temperature, for instance, the addition of 14 w.% Al, the martensitic transformation start will lie around the room temperature. In spite of

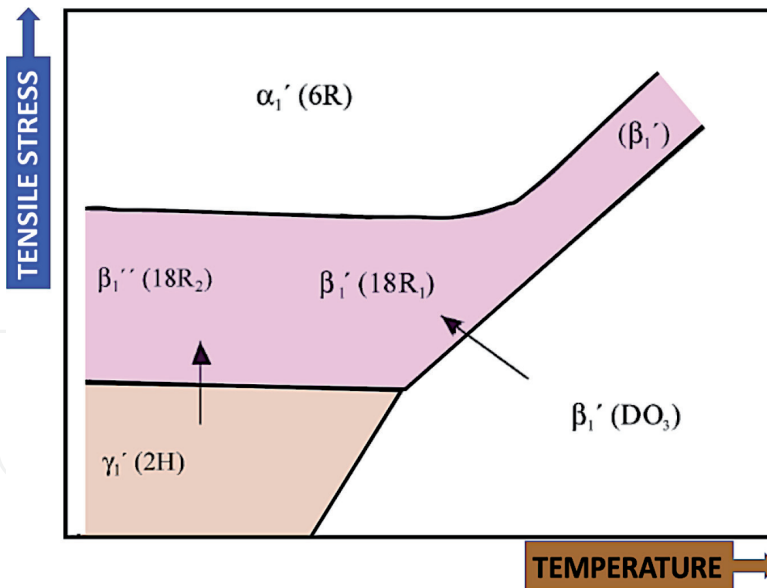


Figure 5. Schematic phase diagram of Cu-Al-Ni alloy in temperature-stress coordinates [1, 30].

this, the Al addition may lead to from new phase known as phase γ_2 (i.e., it refers to the cubic intermetallic compound of Cu_9Al_4), in which it results in increasing the brittleness of the alloy. However, the nickel addition will play an important role of controlling the diffusion rate of Cu into Al, thereby, the may lead to retain single phase of β or β_1 till the martensitic phase transformation starts been reached during the cooling process. From another point of view, increasing the percentages of Ni in the ternary alloy of Cu-Al-Ni SMAs will be a result of the high brittleness associated with shifting the eutectoid point to higher values. Therefore, optimizing the chemical composition of the Al and Ni in the range of 14 and 3.5–4 wt.%, respectively [1]. On the other hand, these alloys still have drawbacks such as low reversible transformation that included the 4% of one-way shape memory effect and 1.5% of two-way shape memory effect. These disadvantages are mainly attributed to the intergranular cracks that occurred at a low stress level. The reasons behind the low stress failure are the large grain size, high elastic anisotropy, intense reliance of transformation strain on crystal orientations as well as segregation on grain boundaries. The first three reasons apply when there is high concentration of shear stress at the grain boundaries. The fourth reason is mainly due to weakening of grain boundaries [33].

3.2 Phase transformation morphology

The martensitic transformation can be induced both thermally and/or through applying an external stress. In other words, applying stress and decreasing the temperature both drive the austenite \rightarrow martensite transformation. In fact, there is a linear relationship between the two forces that is derived from the thermodynamics relationships of the phase transformation, called the Clausius-Clapeyron relationship. Thermal treatments significantly influence the characteristics of the martensitic transformation [34], such as martensite, transformation temperatures and hysteresis, which are very sensitive to the order degree of the β phase and the precipitation process [35, 36]. The copper-based shape memory alloys exhibit a martensitic transformation from the β -phase to a close-packed structure on cooling. Additionally, the high temperatures of the β -phase for the Cu-Al-Ni alloys have a disordered bcc structure similar to the Cu-Zn-Al alloys [37]. In the Cu-Al-Ni alloys, two types of thermally induced martensites (β'_1 and γ'_1) form, depending

on the alloy's composition and heat treatment [38–41]. The stability of the β -phase decreases with decreasing temperature. For example, at a lower temperature, the β -phase can remain metastable under proper cooling (air cooling) [42–44]. The stability limit of the overcooled β -phase must then be established to avoid the expansion of the ordination state of the β -phase and/or the precipitation of the stable phases. However, the improved mechanical properties of Cu-Al-Ni SMA are highly related to the production of alloys with a fine grain size [45]. During the heating-cooling processes, the structure of these alloys' changes within the martensitic region. Moreover, usable forces arise during the martensite \leftrightarrow austenite transformation upon thermal cycling due to the shape recovery properties, which allows these alloys to be used as a component in some devices [46, 47]. The martensitic transformation requires higher energy than the reverse transformation [48].

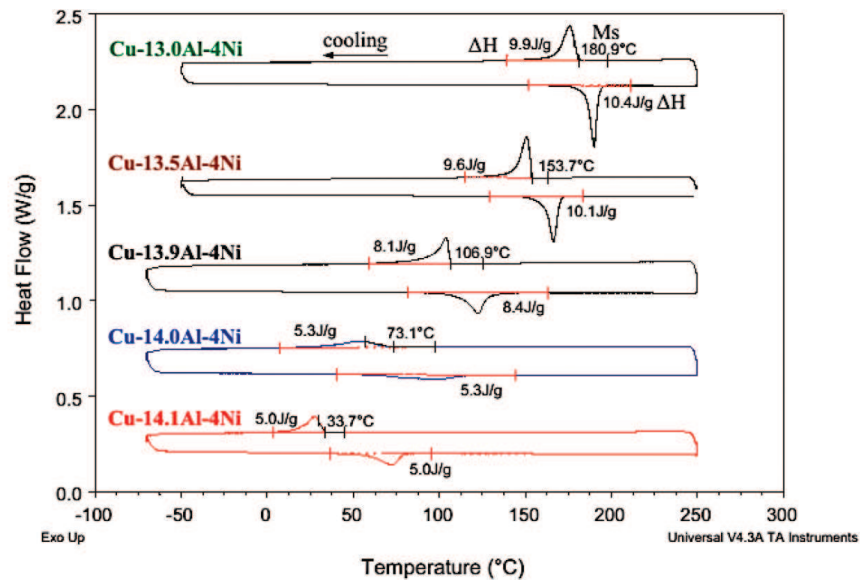
4. Effects of alloying elements on the:

4.1 Martensitic transformation temperature of Cu-Al-Ni SMA

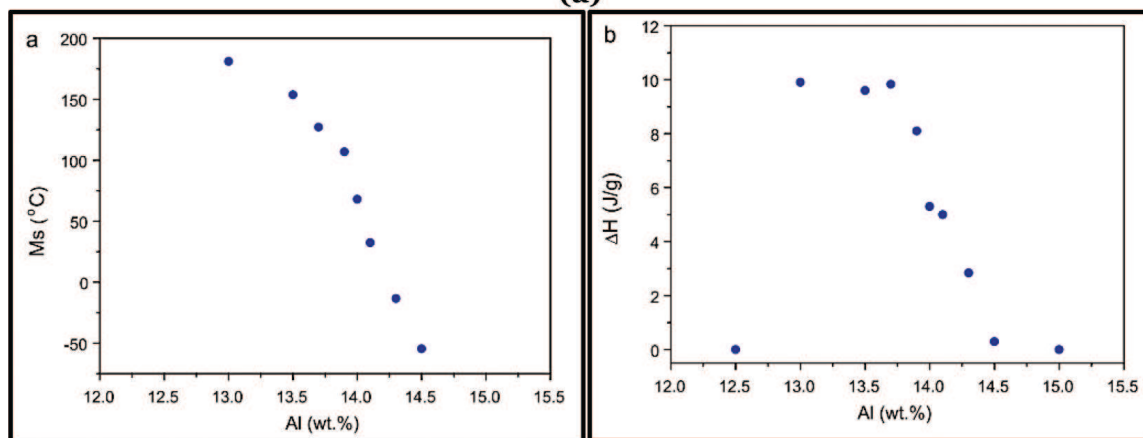
In copper-based shape memory alloys, the most significant factor that controls the martensite transformation is the alloy chemical composition. In commercial applications, the effect of alloying elements on the martensite transformation temperature is highly beneficial during the design of an alloy with the required characteristics [49]. Grain refiners are added to Cu-Al-Ni shape memory alloys for many reasons. These effects are both direct and indirect, such as [50] (i) the transformation temperatures are modified due to the formation of intermetallics; (ii) the remaining solid solution may increase the strength of β phase, thus leading to reduce the M_s and other temperatures; (iii) producing a chemical contribution; and (v) grain growth which occurs during annealing has an influence on the transformation temperatures.

For decreasing brittleness, one of the most important defects of Cu-Al-Ni SMAs, Itsumi et al. [51] replaced 2% of the aluminum content with Mn, which suppressed the eutectoid reaction $\beta_1 \rightarrow \alpha + \gamma_2$; Mn does not decrease the transformation temperature. At the same time, they used 1% of the Ti, which resulted in grain refinement and thus intergranular cracking can be eliminated. Karagoz and Canbay [52] studied the variations of Al and Ni percentages on the phase transformation temperatures, and have found that the forward and reverse transformation temperatures are strongly influenced by the variation of Al wt.%, therefore, higher percentage of Al exhibited lowest transformation temperatures. The variation of Ni wt.% was found to be mainly responsible for suppressing the diffusivity of Cu and Al. Chang [53] found that the M_s temperature of Cu- x Al-4Ni SMAs decreased significantly from 180.9 to -54.7°C when the content of Al was increased from $x = 13.0$ to 14.5 as shown in **Figure 6(a–c)**. This is consistent with the study by Recarte et al. [49], in which the M_s temperature of Cu-Al-Ni SMA depended strongly on its chemical composition, particularly with the content of Al. Cu- x Al-4Ni SMAs with a higher content of Al exhibiting a lower M_s temperature could be ascribed to the fact that the driving force necessary for nucleation of the γ'_1 (2H) martensite is higher than that of the β'_1 (18R) [49, 54, 55].

Sampath [50] found that addition of alloying elements and grain refiners are the main factors that can increase solid solution strengthening, as some of these elements are capable of dissolving into the solution leading to the formation of a second phase. Therefore, with the addition of a minor amount of Ti, Zr, and B to the Cu-Al-Ni SMA, the transformation temperatures are led to increase, as shown in **Figure 7(a–d)**. On the other hand, when the weight percentage of Al and Ni are



(a)



(b)

(c)

Figure 6.

Evolution of (a) DSC heating-cooling curves, (b) the M_s transformation temperature, and (c) the transformation enthalpy of the as a function of Al content [53].

decreased, the transformation temperatures increased. Thus, at less than 12 wt.% of Al, the transformation temperatures are increasing, which is in complete agreement with other researchers [23]. From the same point of view, Miyazaki et al. [56] found that with increase in the amount of Al and Ni in the entire composition of Cu-Al-Ni SMA, the transformation temperatures also tend to decrease. Sugimoto et al. [57] found that with the addition of different percentages of titanium to the Cu-Al-Ni SMA, the transformation temperature are increase. These increases are related to the presence of the X-phase as Ti-rich particles into the microstructure that can reduce the mobility of interfaces between the martensite and β phase. The martensite transformation temperature has behaved according to the type of the alloying element, where it has decreased with increasing Ti amount and increased with increasing the Zr amount as reported by Wayman and Lee [58]. This is attributed to the dissolving percentage of Ti and Zr in the β -phase. Dutkiewicz et al. [59], disagreed that Ti additions decreased the M_s . However, they have proved that the M_s temperature increases as grain size reduces, where the rapid drop of the transformation temperatures is in the smallest grain size range. Saud et al. [60] was shown that the transformation temperature of Cu-Al-Ni SMAs after the addition of Sn which was represented by the exothermic and endothermic curve in **Figure 8**, the results revealed that the behavior of the observed peak tend to be sharp and board at 232 and 350°C, respectively, due to the existence of different types of precipitates that led to limit the stability of the

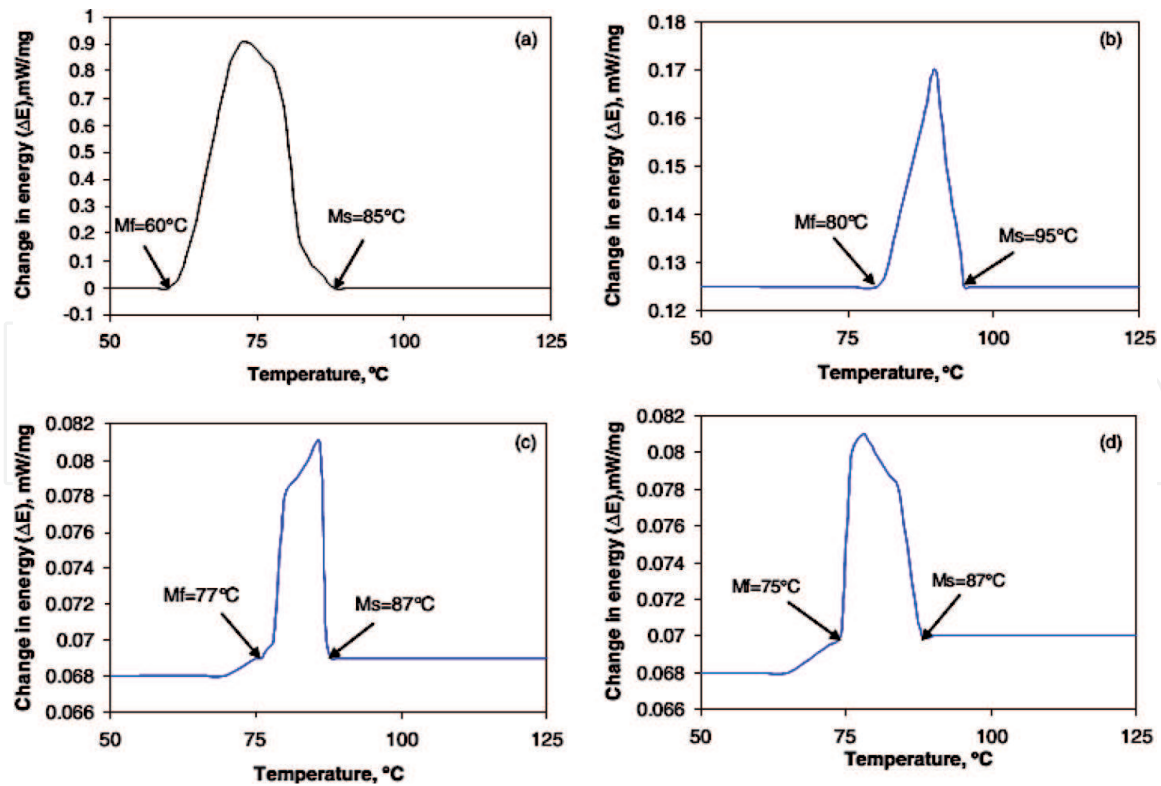


Figure 7. Differential scanning calorimetry profiles for Cu-Al-Ni alloys: (a) Cu-Al-Ni; (b) Cu-Al-Ni-0.2Ti; (c) Cu-Al-Ni-0.4Mn; and (d) Cu-Al-Ni-0.2Zr [50].

low temperature phase and resulted in an individual transformation corresponding to the high driving force.

4.2 Martensitic structure of Cu-Al-Ni SMAs

The sort of thermally introduced martensite is totally dependent primarily on the chemical substance composition of Al and Ni in the Cu-Al-Ni SMAs. Once the martensitic transformation is produced by the deformation loading, the particular martensite acquired is determined by aspects including crystal orientation, chemical compositions of Al/Ni, deformation stress as well as applied temperature. There

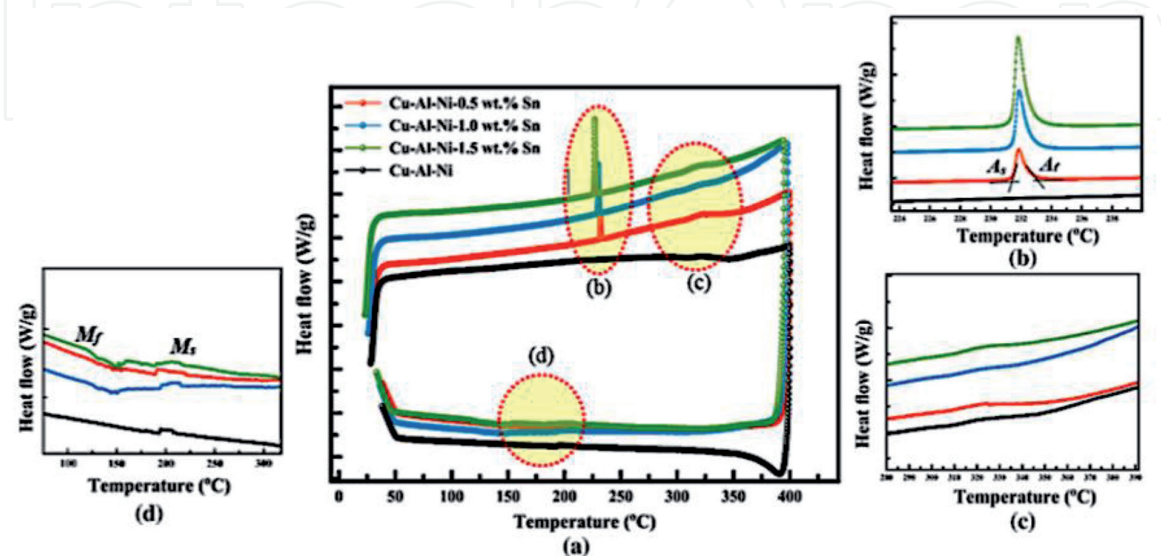


Figure 8. Transformation temperature of Cu-Al-Ni SMAs modified with different percentage of Sn [60]; the magnified peaks of the (a,b) forwards transformation and (c) reverse transformation.

are several reasons behind adding the alloying elements to Cu-based shape memory alloys [50, 61–64], including to (1) refine the grain size, (2) restrict the martensite stabilization, (3) adjust the phase diagrams, (4) accommodate the transformation temperature, (5) improve the workability of these alloys, since they are difficult to process, due to a large grain size having formed during the solidification process, and to enhance the service life of copper shape memory alloys in applications.

The microstructure of Cu-Al-Ni SMA can be formed in a needle and/or plate-like martensites with self-accommodating morphology [50]. Two different phases are excited during adding 13.3% Al and 4.3% Ni to Cu-Al-Ni SMAs: (i) acicular morphology: β'_1 ; and (ii) self-accommodating morphology: γ'_1 . The martensite in Cu-Al-Ni alloy has experienced a gradual transition from β'_1 to γ'_1 via a $\beta'_1 + \gamma'_1$ composition when the percentage of Al increased [49, 65]. At high cooling rate, β martensite transformed to β'_1 martensite with tiny quantities of γ'_1 phase. However, in case of low cooling rate, β'_1 transformed to γ'_1 martensite. The formation of γ'_1 martensite is inevitable irrespective of the processing conditions if the Al content is >14.2 wt.%. Minor additions to the base Cu-Al-Ni alloy tend to produce intermetallic compounds with Al, when the matrix of Al decreases resulting in the formation of β'_1 martensite. If the percentage of Al is less than 11.9 wt.%, large plates of α' martensite will be formed. Fine plates of β'_1 martensite form when the Al content is about 11.9 wt.%. $\beta'_1 + \gamma'_1$ mixtures are observed in Cu-13.03 wt.% Al-4.09 wt.% Ni [66] and martensite formed mainly the M18R type with an orthorhombic structure [67]. However, Chentouf et al. [68] studied the microstructural and thermodynamic analysis of hypoeutectoidal Cu-Al-Ni shape memory alloys and determined that the amount of Al and Ni has a greater effect on the morphology of the precipitated phase as shown in Figure 9.

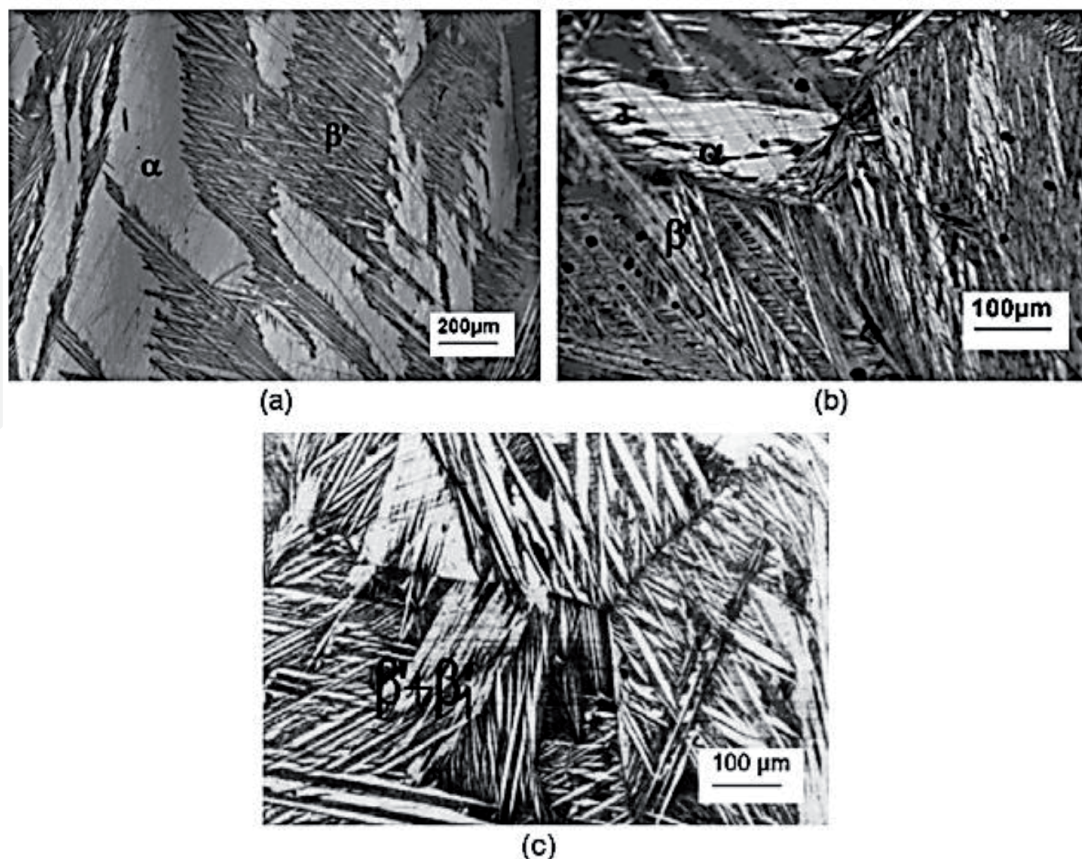


Figure 9.

Optical micrographs for alloys: (a) Cu-9.9 wt.% Al-4.43 wt.% Ni, (b) Cu-11.25 wt.% Al-4.07 wt.% Ni and (c) Cu-11.79 wt.% Al-4.37 wt.% Ni [68].

In Cu-Al-Ni shape memory alloys, large precipitate (X_L) particles are formed resulting in the transformation of the 18R basal plane order into 2H martensite at the interface of the precipitate-free and precipitate-matrix. Ratchev et al. [69] stated that there would be a change in the 18R sequence due to the modification of the stresses around the precipitates. Karagoz and Canbay [52] found that when the percentage of Al addition increased, the β phase leads to the total martensitic transformation of β'_1 and γ'_1 phases during the homogenization process and the grains formed in V-type shape along with different orientations. Chang [53] with 13 wt.% of Al, martensite exhibited self-accommodating zig zag groups at room temperature, whereas the martensite is typical β'_1 martensite with an 18R structure as shown in **Figure 10a**. However, by increasing the Al to 13.5 wt.%, a number of coarse variants of γ'_1 (2H) structure exist in the matrix of β'_1 (18R), as shown in **Figure 10b**. With further increase in the Al amount to 13.7 and 14 wt.%, the microstructure became more distinct exhibiting a β'_1 (18R) or γ'_1 (2H) martensite along with the abundant precipitate of γ_2 phase as demonstrated in **Figure 10c** and **d**. According to the relationship between the variety of transformed martensite and the composition of Cu- x Al-4Ni SMAs reported by Recarte [49, 54, 70], the β'_1 (18R) and the γ'_1 (2H) martensite should coexist in Cu-13.7Al-4Ni SMA, while only γ'_1 (2H) martensite exists in Cu-14.0Al-4Ni SMA.

Sugimoto et al. [57] found that with the addition of Ti to the Cu-Al-Ni SMA, a new phase known as X-phase is going to be formed which is rich in Ti-rich. Also, the volume fraction of this phase is increased linearly with increase in the percentage of Ti addition. Other work has been done by Dutkiewicz et al. [59], where they have agreed that the addition of Ti to the Cu-Al-Ni caused a smaller and elongated grain

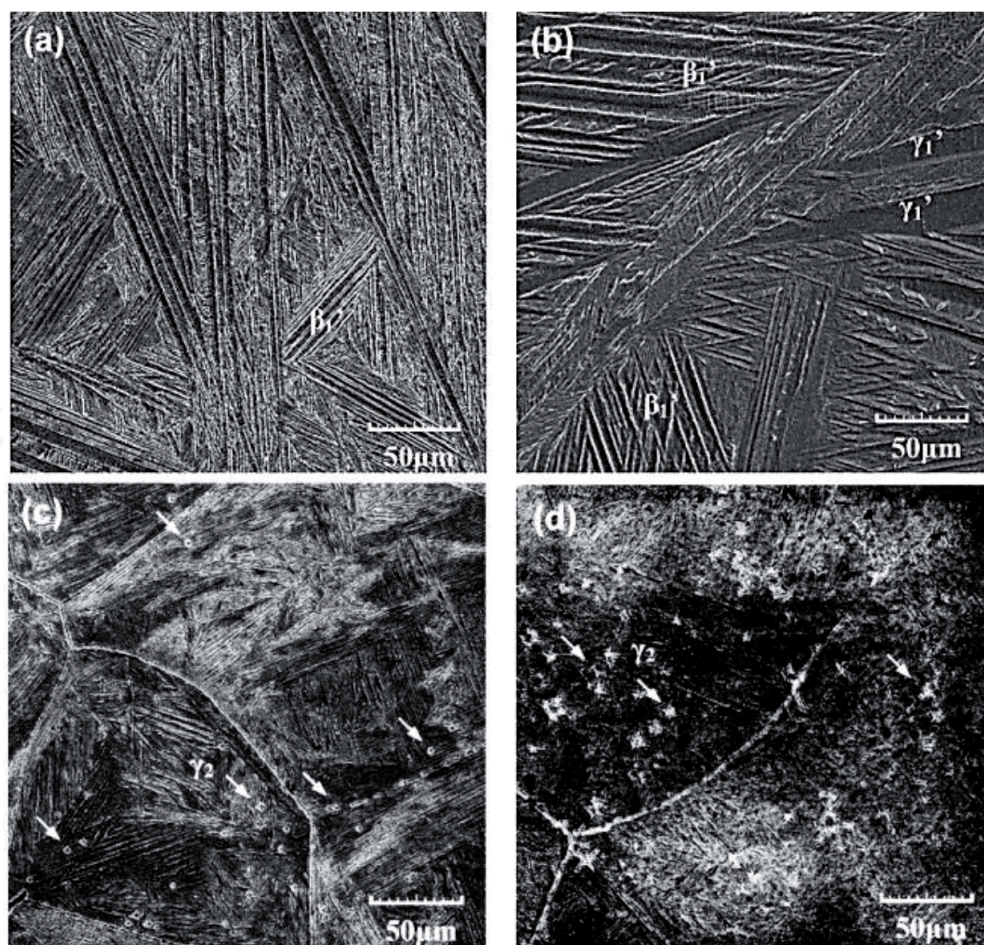


Figure 10. SEM micrographs of (a) Cu-13.0Al-4Ni, (b) Cu-13.5Al-4Ni, (c) Cu-13.7Al-4Ni, and (d) Cu-14.0Al-4Ni SMAs [53].

size because the Ti addition restricted the grain growth as shown in **Figure 11(a–d)**. Font et al. [71] found that the addition of Mn and B along with different thermal cycling have an effect on the parameters on the martensite morphologies and orientations. They found that the martensite formed in two morphologies: plates and thin needles. The plates martensite form as self-accommodation variant groups. However, some particles have been observed to form between the plates and needles and their size is almost same with different amounts of Mn and B added. The distribution of these particles are mainly dependent on the thermal treatment conditions and by using energy dispersive spectroscopy, it was found that these particles are Mn and/or aluminum boride, a result which is in complete agreement with Morris [72]. The existence of these particles is due to difficulties dissolving Mn/B into the matrix. Sampath [50] has shown that two different morphologies are formed into the microstructure of Cu-13.3 wt.% Al-4.3 wt.% Ni SMA and these morphologies are (γ'_1 with a self-accommodating structure and β'_1 with a acicular structure). Also, it was found that with adding a minor addition of Ti, Mn, or Zr to the base alloy, new precipitations/compounds have formed with Al element as shown in **Figure 12(a–d)**. These precipitations are able to enhance the formation of martensite β'_1 phase. Saud et al. [21] presented the changes in the microstructure changes of Cu-Al-Ni SMAs after the addition of different percentages of Ti and the microstructure changes were exhibited in **Figure 13(a–d)**. it was revealed that the presence of γ'_1 and β'_1 phases, on the other hands, there is an irregular phase was observed in the modified microstructure in the shape of flower and it has been formed randomly between β'_1 plates and needles, which this phase was called as X-phase.

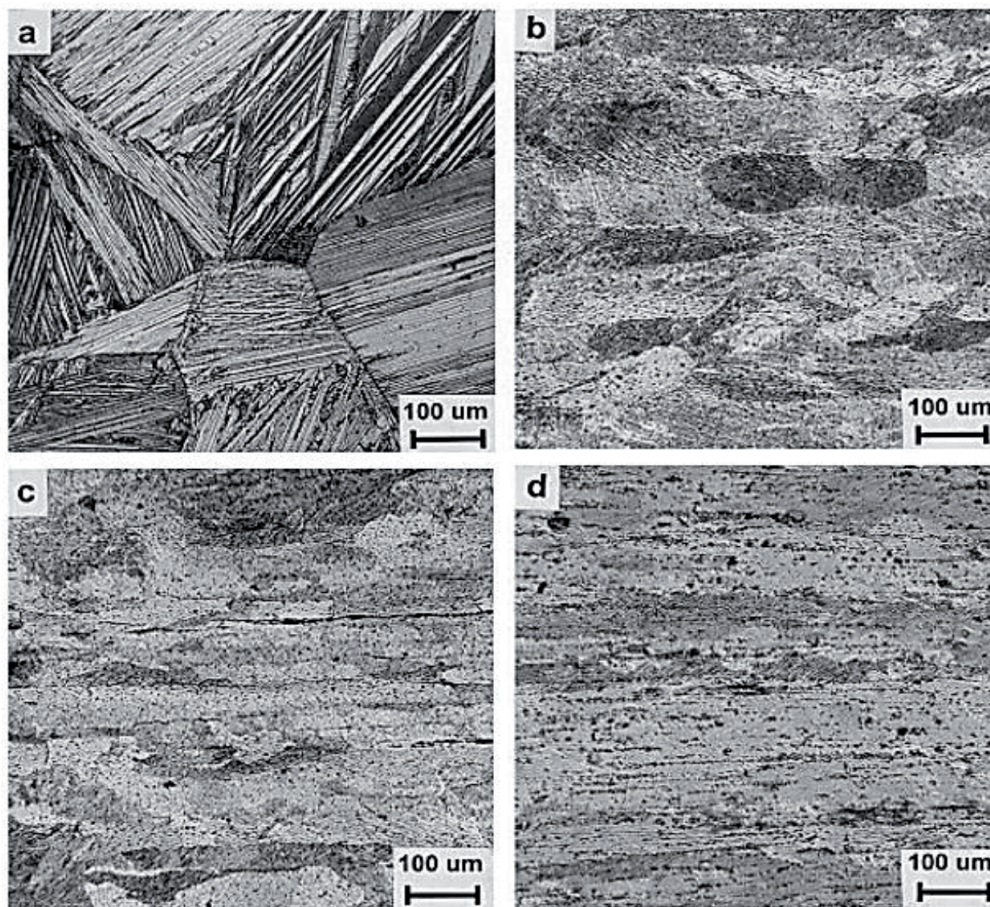


Figure 11. Optical micrographs of (a) Cu-11.85 wt.% Al-3.2 wt.% Ni-3 wt.% Mn, (b) Cu-11.9 wt.% Al-5 wt.% Ni-2 wt.% Mn-1 wt.% Ti, (c) Cu-11.4 wt.% Al-2.5 wt.% Ni-5 wt.% Mn-0.4 wt.% Ti, and (d) Cu-11.8 wt.% Al-5 wt.% Ni-2 wt.% Mn-1 wt.% Ti [59].

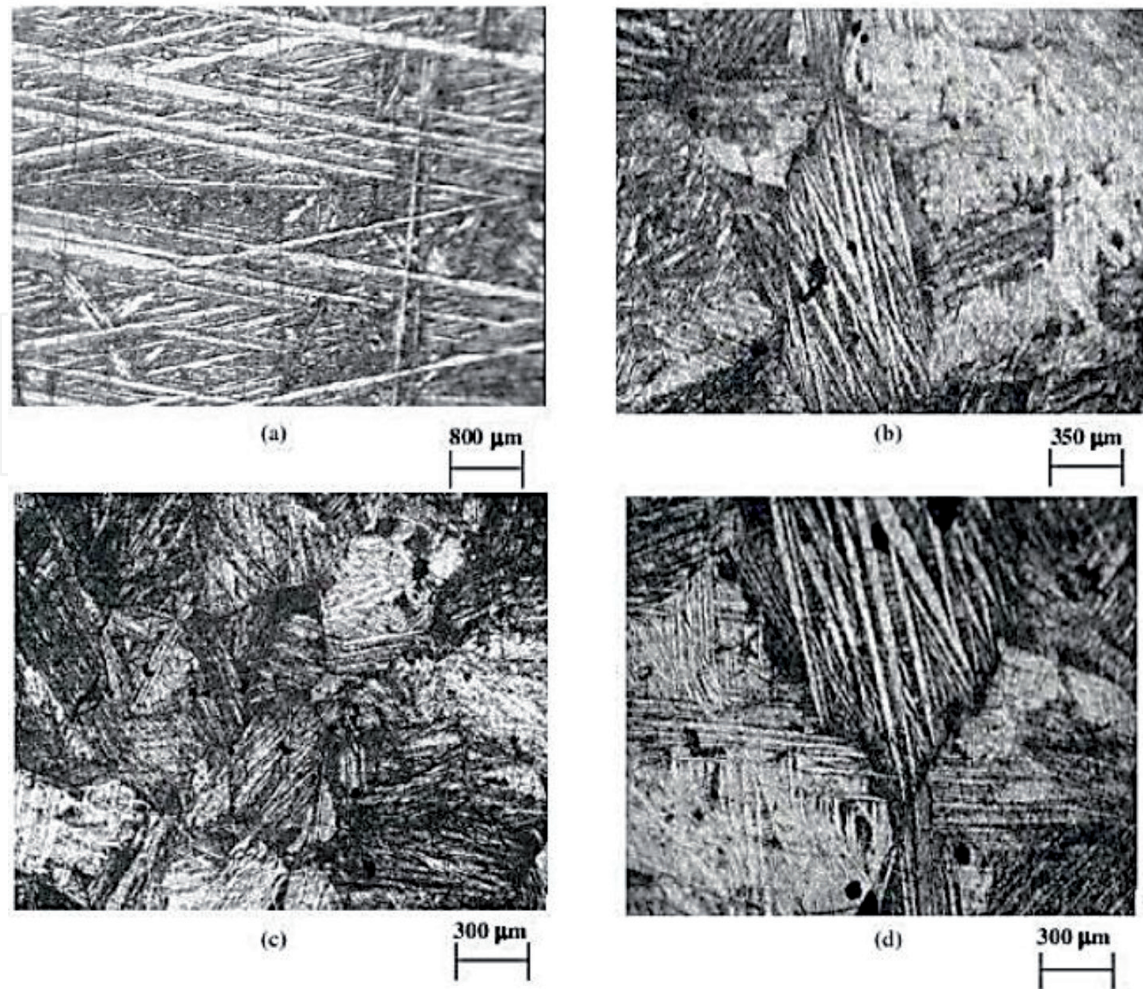


Figure 12.
Optical micrographs of Cu-Al-Ni alloys: (a) Cu-Al-Ni; (b) Cu-Al-Ni-0.2 Ti; (c) Cu-Al-Ni-0.4 Mn; and (d) Cu-Al-Ni-0.2 Zr [50].

4.3 Mechanical properties of Cu-Al-Ni SMA

Cu-Al-Ni shape memory alloys (SMA) have been selected as high potential materials for high temperature applications. This is attributed to their high thermal stability at temperatures above 100°C [73–76]. On the other hand, these alloys have their limitations such as high brittleness because of the appearance of brittle phase γ_2 at grain boundaries, the enormous increase in grain size duplicated with a high elastic variation [77–81]. Thus, their disadvantages have restricted the usage of these alloys for commercial applications [82–92]. One way to solve this problem is the grain refinement. By adding some of the alloying elements such as Ti, Mn, V, Nb, B and others or varying the compositions of Ni or Al, some improvement in mechanical properties of the conventional Cu-Al-Ni SMAs [86, 93–96] was observed. This improvement is attributed to the addition of alloying elements, where these elements are restricting the grain growth and refining the grains. However, these alloying elements have a significant effect on the mechanical properties of Cu-Al-Ni SMAs due to the formation as a second phase structure in the microstructure [97]. Miyzakai et al. [23, 56] found that varying the percentage of Al and Ni lead to changes in crack formation and propagation. It was also found that increases in the Al and Ni amount from 14 and 3.9 wt.% to 14.2 and 4 wt.% lead to the appearance of clear crack formation. This may be attributed to the amount of thermal stress induced and in accordance to the Clausius-Claperyron equation, the increase in the alloying composition of Al and Ni has an effective influence on the

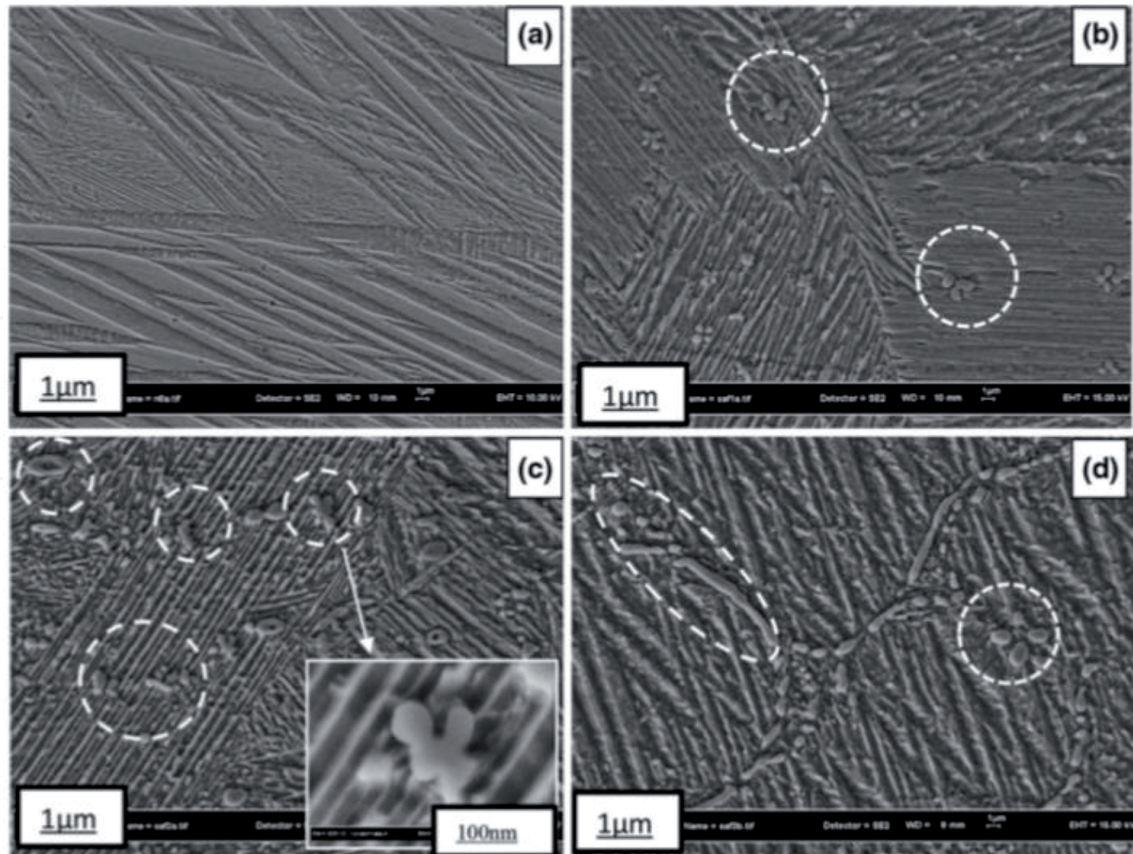


Figure 13.

FESEM micrographs showing the microstructures of the Cu-Al-Ni SMA with different concentration of Ti additions: (a) Cu-Al-Ni (alloy A), (b) Cu-Al-Ni-0.4 mass% Ti (alloy B), (c) Cu-Al-Ni-0.7 mass% Ti (alloy C), (d) Cu-Al-Ni-1 mass% Ti (alloy D) [21].

martensite thermal stress induced, which lead to crack initiation and propagation. The addition of manganese and boron efficiently refine the grain size, however, increasing of the boron concentration produced the highest strain hardening. Wayman and Lee [58] have found that the addition of boride particles helped to relieve the stress concentrations at the grain boundaries. Morris [72] found that by adding the boron to the Cu-Al-Ni SMAs, the ductility increased. This can also be attributed to the presence of boride particle. Another relevant point is that the boron addition can have an effect on the fracture mode, as it has been transferred from brittle failure to intergranular and transgranular failure. Another work by the same author [98], found that the values of yield stress, hardness and tensile

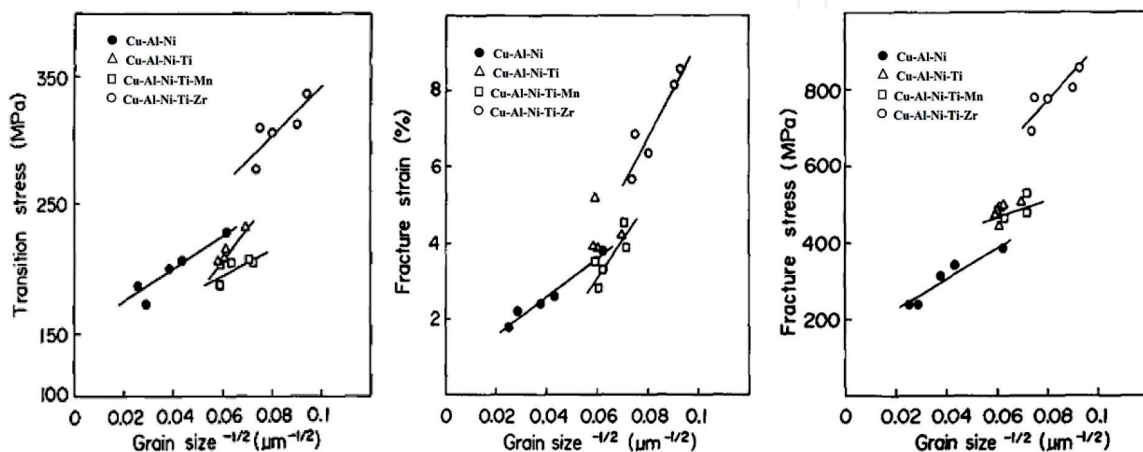


Figure 14.

Variation in the (a) transition stress, (b) fracture strain, and (c) fracture stress versus grain size [99].

strength have been increased with increasing the percentage of boron addition. It seems that the boride particles have restricted the interface movement, therefore the required stress to re-orient the martensite phase is high. These particles have played a significant role by accommodating a new strain concentration generated by the coexistence of the new stress-induced martensite. Roh et al. [99] reported that the fine grained alloys resulting from the addition of Ti, Mn, and Zr to the coarse grained Cu-Al-Ni SMA lead to enhance the fracture stress-strain. It was found that the fracture stress and strain obtained the highest value of 930 MPa and 8.6%, respectively, with the combined addition of 0.3Ti-0.6Zr to Cu-13.4Al-3.05Ni SMA. This improvement is due to grain refinement and the presence of precipitates that formed within grains in the alloy. They have also confirmed other researchers' findings [86, 100, 101] that the tensile properties of (σ_t , σ_f , and ϵ_t) increased as a function of decreasing grain size, as shown in **Figure 14**. In contrast, the fractured surfaces of Cu-Al-Ni SMA changed from brittle mode to different modes according to the type and amount of the addition element as shown in **Figure 15**.

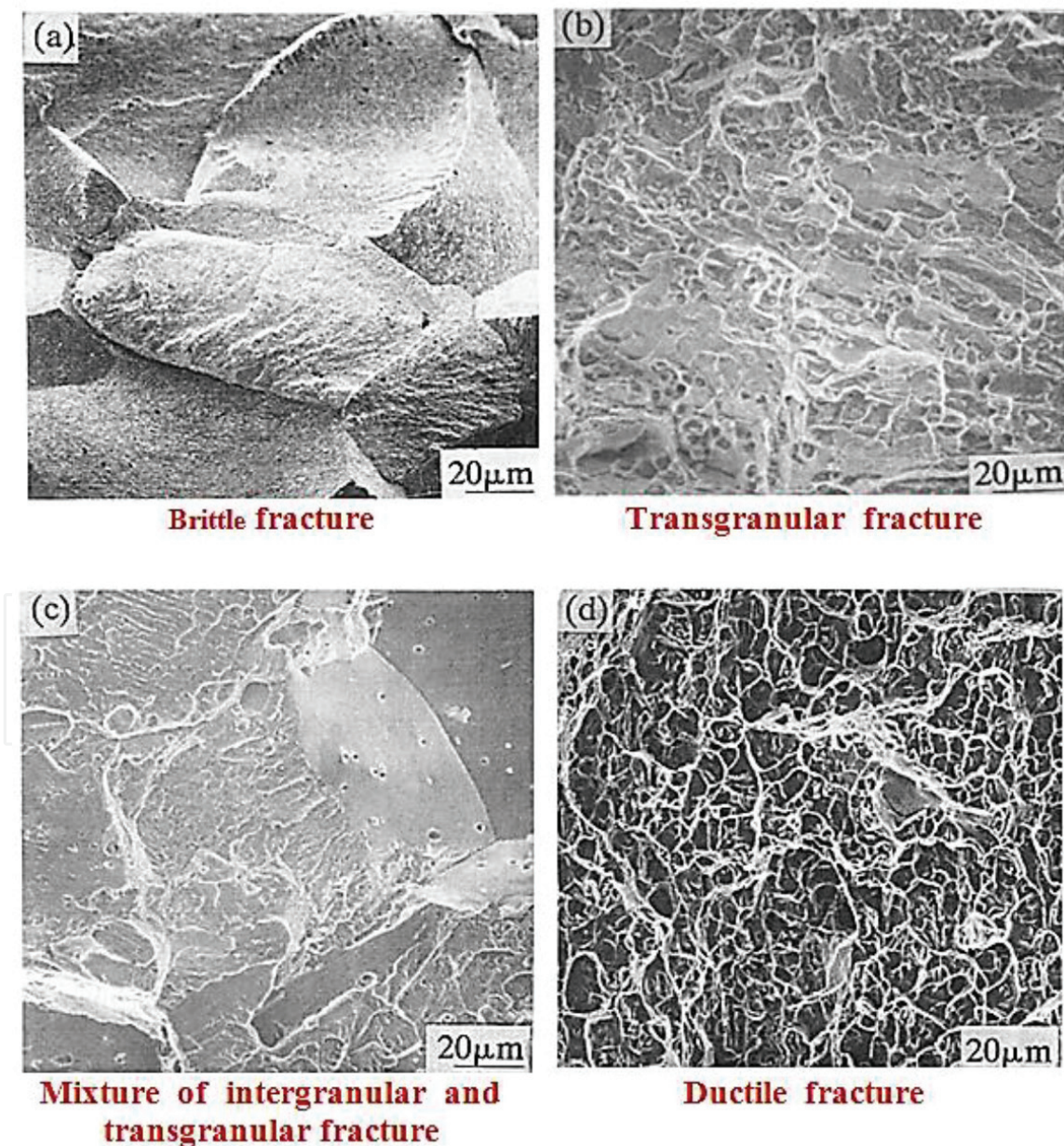


Figure 15. Tensile fracture surfaces at room temperature for (a) Cu-13.4Al-3.8Ni SMA, (b) Cu-13.2Al-3.04Ni-0.36Ti SMA, (c) Cu-13.0Al-2.9Ni-0.36Ti-0.22Mn SMA and (d) Cu-13.4Al-3.05Ni-0.24Ti-0.63Zr SMA [99].

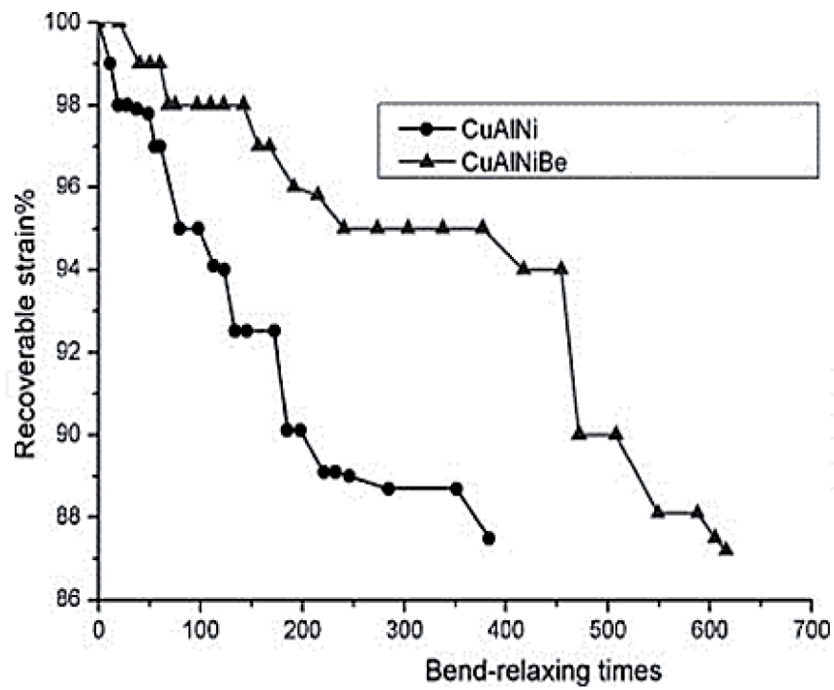


Figure 16. Recoverable strain versus bend-relaxing time of Cu-Al-Ni and Cu-Al-Ni-Be [105].

Xu et al. [102, 103] found by adding the Be to the Cu-Al-Ni SMAs, the fatigue life has been increased, as the strain recovery has reached 30% higher than base alloy. Increase in the recovery strain is almost equal to the recovery strain of the NiTi. Zhu et al. [97] found the bending performance, tensile strength, and elongation percentage of Cu-Al-Ni-Be are higher than Cu-Al-Ni alloy, where the maximum stress of this alloy could reach to 780 MPa with 18% of strain as shown in **Figures 16** and **17**. This may imply that the mechanical property of Cu-based SMAs can be significantly improved by adding the alloying elements. The additions of Ti, Mn, and Zr to Cu-Al-Ni shape memory alloys have decreased the grain size reported by Sampath [50], therefore the values of hardness increased. This is attributed to the formation of fine precipitates that

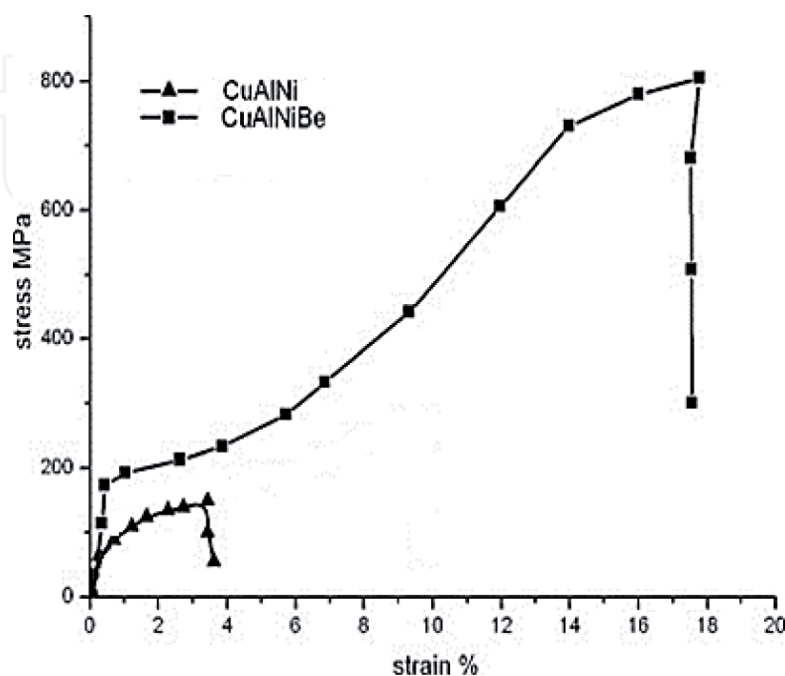


Figure 17. Stress-strain curves of SMA samples at room temperature (25°C) [105].

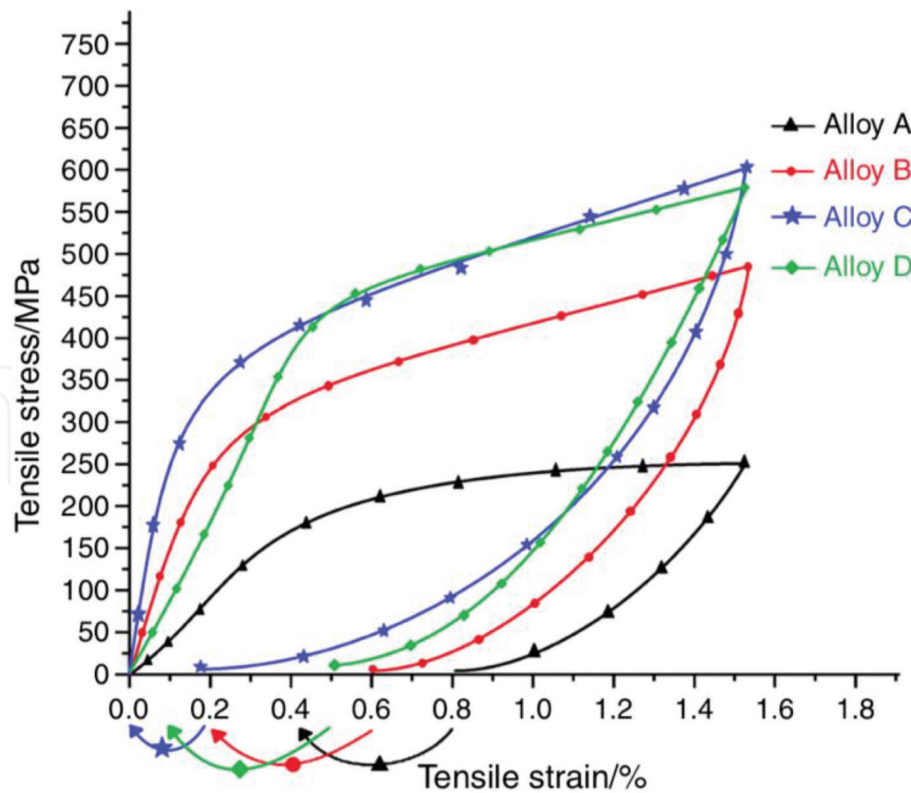


Figure 18. Shape memory effect curves of the alloys performed at $T < M_s$ then preheated to $T > A_f$ to obtain the shape recovery [21], Cu-Al-Ni (alloy A), Cu-Al-Ni-0.4 mass% Ti (alloy B), Cu-Al-Ni-0.7 mass% Ti (alloy C), Cu-Al-Ni-1 mass% Ti (alloy D).

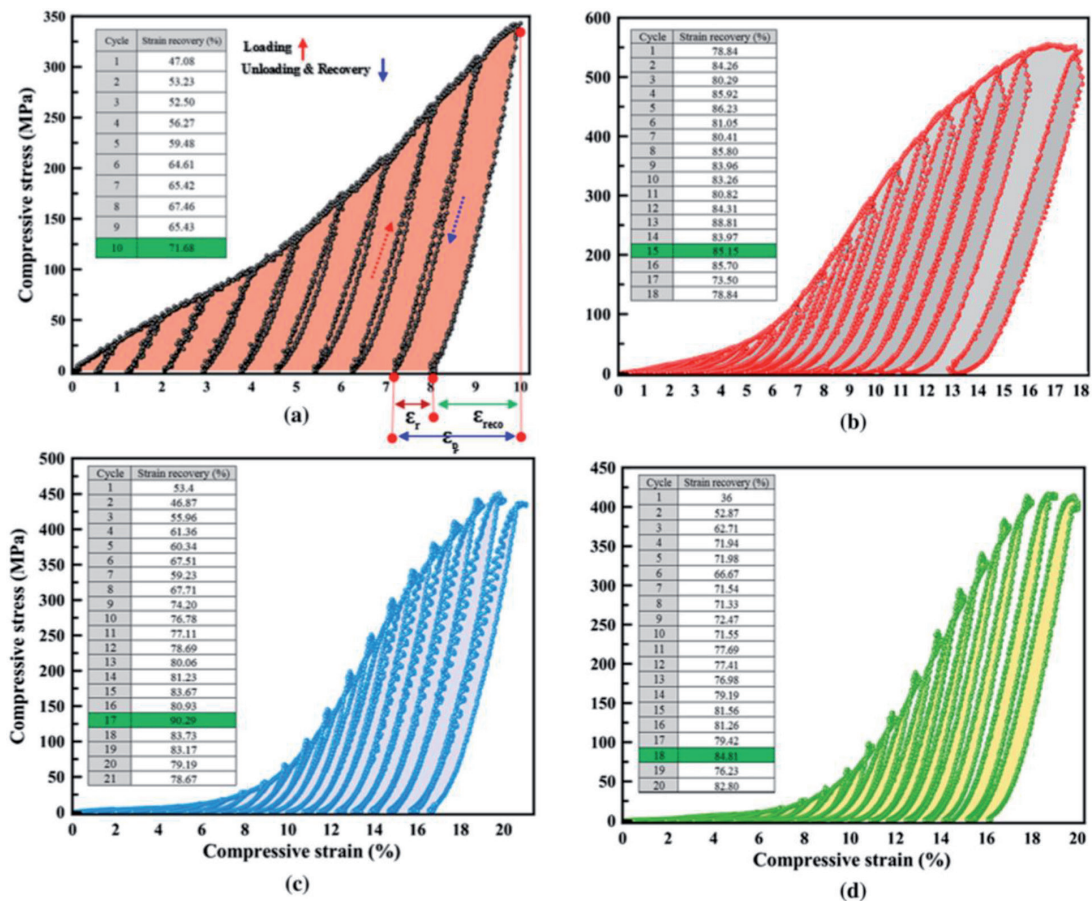


Figure 19. Compressive stress–strain of different loading–unloading cycles tested at a temperature of 473 K (200°C); (a) Cu-Al-Ni; (b) Cu-Al-Ni-0.5 wt.% Sn; (c) Cu-Al-Ni-1.0 wt.% Sn; and (d) Cu-Al-Ni-1.5 wt.% Sn [60].

restricted the grain growth by the pinning effect. Also, other elements have shown a significant effect on the mechanical properties of Cu-Al-Ni SMAs during the addition. For example, the rupture strain of Nb and V has increased up to 14 and 6%, respectively, which is much higher than the base alloy as reported by Gomes et al. [104]. The strain recovery by the shape memory effect (ϵ_{SME}) of the Cu-Al-Ni SMAs with and without the Ti additions was studied by Saud et al. [21], as shown in **Figure 18**. The results were shown that the addition of Ti with different mass percentages exhibited an increase in the values of strain recovery by the SME. These enhancements in references the strain recovery were attributed to the existence of the X-phase that was brought about by the Ti additions in the parent phase. Another study by the same authors [60] shown the effect of different percentage of 0.5, 1.0, and 1.5 wt.% of Sn addition on the stress-strain curves under multi-cycles of loading and unloading. It was found that the largest number of cycles was indicated with the Cu-Al-Ni-1 wt.%Sn SMA before the occurrence of fracture, as shown in **Figure 19(a-d)**. This improvement is due to two reasons: low porosity density and the finest particle size among the alloys.

5. Brief applicability of Cu-based SMAs

Predominantly, the shape memory applications can be separated into four classes as per the essential capacity of their memory component [106–109] where the SME can be utilized to create movement as well as load, and the SE can store the twisting vitality [110, 111]. The extraordinary conduct of SMAs has produced new applications in the aviation, automobile, robotization, and control, machine, vitality, synthetic handling, warming and ventilation, security and safety, and hardware (MEMS gadgets) ventures. A part of these applications applies comparative strategies, ideas or systems, which are additionally relevant for different regions. Most of these plausible applications are secured with the economically accessible parallel Nitinol SMA, where its operational temperature run lies around inside the standard scope of ecological temperature boundaries to which a traveler vehicle might be uncovered amid administration, for example, between -40°C to approx. $+125^{\circ}\text{C}$ [112, 113]. The binary alloy system of NiTi SMA with change temperatures from -50°C to approximately to $+110^{\circ}\text{C}$ [106] performs well for various cycles inside vehicle areas in varies range of performing temperatures [113, 114], however not in areas with higher temperatures, for example, under the motor hood. The SMAs ought to have a martensite finish temperature well over the most extreme working temperatures (see the dark spotted lines in **Figure 20**) so as to work appropriately. The correlation of the change temperature scopes of the most widely recognized SMAs that the less expensive Cu-Al-Ni SMAs can play out the change with temperatures up to 200°C , however, these SMAs are fragile, unsteady, have low exhaustion quality and are not appropriate for numerous cyclic activities [106, 113, 115–119]. A wide determination of high temperature SMAs are accessible, however, these materials are known as costly for automobile applications [113].

Since the 1980s, SMAs have been used in many different robotic systems, especially as micro-actuators or artificial muscles [123–125] as described by Furuya and Shimada [126] and Sreekumar et al. [127]. Today, most of the SMA robotic applications were biologically inspired (i.e., biomechanics) and widely utilized in biomedical areas but are also used extensively in other fields as well. The difficulties are to expand the execution and scaling down of the equipment stage and to build the insight of the coordinated framework (for example small-sizes, consistent and self-controlling). A few specialized issues were featured and should be settled, for example, clamping difficulties, miniature electrical connection (for micro robots), small strain, control issues and very low efficiency. Besides, part of these issues

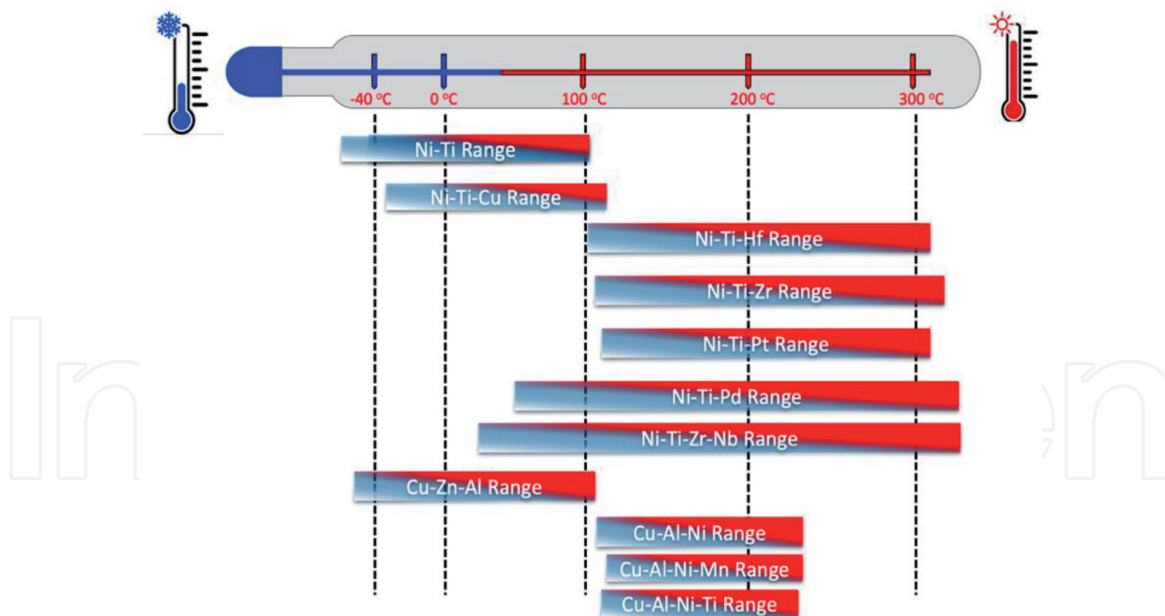


Figure 20.

Operating temperature range for automobiles applications and the transformation temperatures for selected commercially available and developed SMAs [106, 113, 120–122].

has been controlled by choosing an appropriated modeling strategy as sensor to control and feedback. For instance, the control of resistance feedback is perfect for small scale robots as it takes out the additional requirement for extra sensors, in spite of the fact that the obtained limited accuracy [127]. Earlier, it was found that the response of the SMA actuator is mainly relying on structural design and thus limited the robotic functionalities in terms of the degree of freedom (DOF). On the other hands, the heating resistivity is a common technique been implemented for a micro-size SMA actuators, however, macro-size actuators are required to a direct heating source to acquire the shape memory features. In addition to enhance the frequency of the actuators, a capacitor will be attached for a faster heating response along with above-mentioned cooling methods that resulted in larger device shape [127]. Another problem to be mentioned that the complexity of the control system that found due to the large numbers of actuator were employed to increase the robots DOF.

Another significant implementation for shape memory as absorbers in bridges that been effectively used [128, 129]. According to the study was carried out by European Union on the earthquake damages and the way of finding a sustainable technology to prevent the disaster damage via seismic vibration. A research was conducted for as modeling for four story building, which was constructed using the tendons techniques to minimize the earthquake possible damage, where it was found that the building without SMA was completely destroyed while the incorporated building with SMA got less damage, whereby, the implemented tendons were used to absorb energy based on the shape memory feature of super-elastic behavior and reduced the shocked waves of earthquake.

6. Summary

In this chapter the characteristic of shape memory alloys in terms of microstructure, mechanical properties and thermal cyclic stress-strain curves of Cu-Al-Ni SMAs. The main benefits of these alloys can be obtained after the modifications were made, as, for a certain application, the selective of shape memory alloys

required the main consideration in term of manufacturing cost and performance, thus the Cu-Al-Ni SMAs have been shown interested attentions due to their low cost compared with Ti-based shape memory alloys. However, many researchers have faced a challenge when Cu-based shape memory materials are used for in many applications, due to their limitations such as the high brittleness and low recovery strain, thereby these properties need to be improved. Therefore, modifying the microstructure and the phase characteristics via adding the alloying elements may represent a more significant solution. The addition of the fourth element to the ternary alloy of Cu-Al-Ni SMA is able to alter the structure and/or morphology of the martensitic phase and thus improve the mechanical properties.

Acknowledgements

The author would like to thank the Management and Science University (MSU) for providing the research support under the Seed Research Grant No. SG-451-0518-ISE.

Conflict of interest

The authors declared without any conflict of interest.

Author details

Safaa Najah Saud Al-Humairi
Faculty of Information Sciences and Engineering, Management and Science
University, Shah Alam, Selangor, Malaysia

*Address all correspondence to: safaaengineer@gmail.com

IntechOpen

© 2019 The Author(s). Licensee IntechOpen. This chapter is distributed under the terms of the Creative Commons Attribution License (<http://creativecommons.org/licenses/by/3.0>), which permits unrestricted use, distribution, and reproduction in any medium, provided the original work is properly cited. 

References

- [1] Otsuka K, Wayman CM. Shape Memory Materials. Reprint. Illustrated ed. London, UK: Cambridge University Press; 1999
- [2] Gardan J. Smart materials in additive manufacturing: State of the art and trends. *Virtual and Physical Prototyping*. 2019;**14**(1):1-18
- [3] Farag SG. Application of smart structural system for smart sustainable cities. In: 4th MEC International Conference on Big Data and Smart City (ICBDSC). USA: IEEE; 2019
- [4] Morales-Rivas L et al. Crystallographic examination of the interaction between texture evolution, mechanically induced martensitic transformation and twinning in nanostructured bainite. *Journal of Alloys and Compounds*. 2018;**752**:505-519
- [5] Wu S et al. Mechanical properties of low-transformation-temperature weld metals after low-temperature postweld heat treatment. *Science and Technology of Welding and Joining*. 2019;**24**(2):112-120
- [6] Vokoun D, Kafka V. Mesomechanical modeling of shape memory effect. In: *Symposium on Smart Structures and Materials*. California, USA: International Society for Optics and Photonics; 1999
- [7] Malinin V et al. Development of methods of structural-analytical mesomechanics that take into account the statistical properties of martensitic transformations in materials with shape memory effect. In: *IOP Conference Series: Materials Science and Engineering*. Bristol, England: IOP Publishing; 2018
- [8] Yu C et al. A micromechanical model for the grain size dependent super-elasticity degeneration of NiTi shape memory alloys. *Mechanics of Materials*. 2018;**125**:35-51
- [9] Kumar P, Lagoudas D. *Introduction to Shape Memory Alloys*. United States: Springer; 2008
- [10] Mohammed MT, GEETHA M. Effect of thermo-mechanical processing on microstructure and electrochemical behavior of Ti–Nb–Zr–V new metastable β titanium biomedical alloy. *Transactions of Nonferrous Metals Society of China*. 2015;**25**(3):759-769
- [11] Nishiyama Z, Fine ME, Wayman CM. *Martensitic Transformation*. United States: Academic Press; 1978
- [12] Mori M et al. Tuning strain-induced γ -to- ε martensitic transformation of biomedical Co–Cr–Mo alloys by introducing parent phase lattice defects. *Journal of the Mechanical Behavior of Biomedical Materials*. 2019;**90**:523-529
- [13] Wang J et al. New insights on nucleation and transformation process in temperature-induced martensitic transformation. *Materials Characterization*. 2019;**151**:267-272
- [14] Popov PA. *Constitutive Modelling of Shape Memory Alloys and Upscaling of Deformable Porous Media*. United States: Texas A&M University; 2005
- [15] Patoor E et al. Shape memory alloys, part I: General properties and modeling of single crystals. *Mechanics of Materials*. 2006;**38**(5):391-429
- [16] Lagoudas DC. *Shape Memory Alloys: Modeling and Engineering Applications*. United States: Springer; 2008
- [17] Saburi T et al. The shape memory mechanism in 18R martensitic alloys. *Acta Metallurgica*. 1980;**28**(1):15-32

- [18] Alkan S et al. Transformation stress of shape memory alloy CuZnAl: Non-Schmid behavior. *Acta Materialia*. 2018;**149**:220-234
- [19] Carpinteri A et al. Mechanical behaviour and phase transition mechanisms of a shape memory alloy by means of a novel analytical model. *Acta Mechanica et Automatica*. 2018;**12**(2):105-108
- [20] Lagoudas DC. *Shape Memory Alloys and Engineering Applications*. New York: Springer; 2008
- [21] Saud S et al. Influence of Ti additions on the martensitic phase transformation and mechanical properties of Cu–Al–Ni shape memory alloys. *Journal of Thermal Analysis and Calorimetry*. 2014;**118**(1):111-122
- [22] Tadaki T. *Cu-based shape memory alloys. Shape memory materials*. United Kingdom: Cambridge University Press; 1998. p. 97-116
- [23] Miyazaki S, Kawai T, Otsuka K. Study of fracture in Cu-Al-Ni shape memory bicrystals. *Le Journal de Physique Colloques*. 1982;**43**:C4, C4-813-C4-818
- [24] Horikawa H et al. Orientation dependence of $\beta_1 \rightarrow \beta_1'$ stress-induced martensitic transformation in a Cu-Al-Ni alloy. *Metallurgical Transactions A*. 1988;**19**(4):915-923
- [25] Otsuka K, Sakamoto H, Shimizu K. Successive stress-induced martensitic transformations and associated transformation pseudoelasticity in Cu-Al-Ni alloys. *Acta Metallurgica*. 1979;**27**(4):585-601
- [26] Eisenwasser J, Brown L. Pseudoelasticity and the strain-memory effect in Cu-Zn-Sn alloys. *Metallurgical Transactions*. 1972;**3**(6):1359-1363
- [27] Lexcellent C. *Shape-Memory Alloys Handbook*. New Jersey, United States: Wiley; 2013
- [28] Dunne NFKADP. Shape strains associated with thermally-induced and stress-induced martensite in a Cu-Al-Ni shape memory alloy. *Acta Metallurgica*. 1982;**30**:429-435
- [29] Chen Y et al. Shape memory and superelasticity in polycrystalline Cu–Al–Ni microwires. *Applied Physics Letters*. 2009;**95**(17):171906
- [30] Delaey L. Diffusionless transformations. In: Cahn RW, Haasen P, Kramen EJ, editors. *Phase Transformations in Materials, Material Science and Technologies*. New York: VCH Publishers; 1990. pp. 339-404
- [31] Mavroidis C, Pfeiffer C, Mosley M. 5.1 conventional actuators, shape memory alloys, and electrorheological fluids. *Automation, Miniature Robotics, and Sensors for Nondestructive Testing and Evaluation*. 2000;**4**:189
- [32] Scherngell H. Stability and Optimization of the Two-Way Effect in Ni–Ti and Cu–Al–Ni Shape Memory Alloys. *Montanuniversit: Leoben*; 2000
- [33] Miyazaki S, I.C.f.M. Sciences. In: Fremond M, Miyazaki S, editors. *Shape Memory Alloys*. United States: Springer; 1996
- [34] Zhang Xiangyang SQ, Shouwen Y. A non-invariant plane model for the interface in CuAlNi single crystal shape memory alloys. *Journal of the Mechanics and Physics of Solids*. 2000;**48**:2163-2182
- [35] Nó ML, Caillard D, San Juan J. A TEM study of martensite habit planes and orientation relationships in Cu–Al–Ni shape memory alloys using a fast Δg -based method. *Acta Materialia*. 2009;**57**(4):1004-1014
- [36] Qiao L et al. Nonlocal superelastic model of size-dependent hardening and dissipation in single crystal Cu-Al-Ni shape memory alloys. *Physical Review Letters*. 2011;**106**(8):085504

- [37] Xu JW. Effects of Gd addition on microstructure and shape memory effect of Cu–Zn–Al alloy. *Journal of Alloys and Compounds*. 2008;**448**(1-2):331-335
- [38] MLaRR C. Isothermal decomposition of some β Cu–Zn–Al alloys with $e/a=1.48$. *Materials Science and Engineering A*. 1999;**273**-275:577-580
- [39] Agrawal A, Dube RK. Methods of fabricating Cu–Al–Ni shape memory alloys. *Journal of Alloys and Compounds*. 2018;**750**:235-247
- [40] Saud SN et al. Effects of quenching media on phase transformation characteristics and hardness of Cu–Al–Ni–Co shape memory Alloys. *Journal of Materials Engineering and Performance*. 2015;**24**(4):1522-1530
- [41] Gustmann T et al. Properties of Cu-based shape-memory alloys prepared by selective laser melting. *Shape Memory and Superelasticity*. 2017;**3**(1):24-36
- [42] Gera DB et al. The influence of sintering parameters in the microstructure and mechanical properties of a Cu–Al–Ni–Mn–Zr shape memory alloy. *Advanced Engineering Materials*. 2018;**20**(10):1800372
- [43] Velmurugan C, Senthilkumar V. The effect of Cu addition on the morphological, structural and mechanical characteristics of nanocrystalline NiTi shape memory alloys. *Journal of Alloys and Compounds*. 2018;**767**:944-954
- [44] Li D-Y et al. Superelasticity of Cu–Ni–Al shape-memory fibers prepared by melt extraction technique. *International Journal of Minerals, Metallurgy, and Materials*. 2016;**23**(8):928-933
- [45] Otsuka K, Saxena A, Deng J, Ren X. Mechanism of the shape memory effect in martensitic alloys: An assessment. *Philosophical Magazine*. 2011;**91**(36):4514-4535
- [46] Bayram Ü, Maraşlı N. Thermal conductivity and electrical resistivity dependences on growth rate in the directionally solidified Al–Cu–Ni eutectic alloy. *Journal of Alloys and Compounds*. 2018;**753**:695-702
- [47] Braga FO et al. Martensitic transformation under compression of a plasma processed polycrystalline shape memory CuAlNi alloy. *Materials Research*. 2017;**20**(6):1579-1592
- [48] Wei ZG, Peng HY, Yang DZ, Chung CY, Lai JKL. Reverse transformations in CuAlNiMnTi alloy at elevated temperatures. *Acta Materialia*. 1996;**44**(3):1189-1199
- [49] Recarte V et al. Dependence of the martensitic transformation characteristics on concentration in Cu–Al–Ni shape memory alloys. *Materials Science and Engineering: A*. 1999;**273**:380-384
- [50] Sampath V. Studies on the effect of grain refinement and thermal processing on shape memory characteristics of Cu–Al–Ni alloys. *Smart Materials and Structures*. 2005;**14**(5):S253-S260
- [51] Itsumi Y, Miyamoto Y, Takashima T, Kamei K, Sugimoto K. The effects of ageing on the martensitic transformation temperature in Cu–Al–Ni–Mn–Ti shape memory alloys. *Advanced Materials Research*. 1991;**56-58**:469-474
- [52] Karagoz Z, Canbay CA. Relationship between transformation temperatures and alloying elements in Cu–Al–Ni shape memory alloys. *Journal of Thermal Analysis and Calorimetry*. 2013;**114**(3):1069-1074

- [53] Chang SH. Influence of chemical composition on the damping characteristics of Cu–Al–Ni shape memory alloys. *Materials Chemistry and Physics*. 2011;**125**(3):358-363
- [54] Recarte V et al. Study by resonant ultrasound spectroscopy of the elastic constants of the β phase in Cu–Al–Ni shape memory alloys. *Materials Science and Engineering: A*. 2004;**370**(1-2):488-491
- [55] Recarte V et al. Vibrational and magnetic contributions to the entropy change associated with the martensitic transformation of Ni–Fe–Ga ferromagnetic shape memory alloys. *Journal of Physics. Condensed Matter*. 2010;**22**(41):416001
- [56] Miyazaki S et al. The fracture of Cu–Al–Ni shape memory alloy. *Transactions of the Japan Institute of Metals*. 1981;**22**(4):244-252
- [57] Sugimoto K et al. Grain-refinement and the related phenomena in quaternary Cu–Al–Ni–Ti shape memory alloys. *Le Journal de Physique Colloques*. 1982;**43**(C4):C4-761-C4-766
- [58] Wayman CM, Lee JS. Grain refinement of a Cu–Al–Ni shape memory alloys by Ti and Zr additions. *Transactions of Japan Institute of Metals*. 1986;**27**(8):584-591
- [59] Dutkiewicz J, Czeppe T, Morgiel J. Effect of titanium on structure and martensitic transformation in rapidly solidified Cu–Al–Ni–Mn–Ti alloys. *Materials Science and Engineering: A*. 1999;**273**:703-707
- [60] Saud SN et al. Influence of tin additions on the phase-transformation characteristics of mechanical alloyed Cu–Al–Ni shape-memory alloy. *Metallurgical and Materials Transactions A*. 2016;**47**(10):5242-5255
- [61] van Humbeeck J, Chandrasekaran M, Stalmans R. Copper-based shape memory alloys and the martensitic transformation. *Proceedings of the International conference on Martensite Transformation*. 1993;**25**:1015
- [62] van Humbeeck J, Chandrasekaran M, Stalmans R. Shape memory alloys, types and functionalities. In: *Encyclopedia of Smart Materials*. United States: John Wiley & Sons, Inc; 2002
- [63] Chen X et al. Microstructure, superelasticity and shape memory effect by stress-induced martensite stabilization in Cu–Al–Mn–Ti shape memory alloys. *Materials Science and Engineering: B*. 2018;**236**:10-17
- [64] Guzik AT, Benafan O. Design and Development of CubeSat Solar Array Deployment Mechanisms Using Shape Memory Alloys. In: *44th Aerospace Mechanisms Symposium*. Ohio: NASA/TM; 16-18 May 2018. pp.219914
- [65] Bhattacharya B, Bhuniya A, Banerjee MK. Influence of minor additions on characteristics of Cu–Al–Ni alloy. *Materials Science and Technology*. 1993;**9**:654-665
- [66] Chen C, Liu T. Phase transformations in a Cu–14.2 Al–7.8 Ni alloy. *Metallurgical and Materials Transactions A*. 2003;**34**(3):503-509
- [67] Duerig TW et al. *Engineering Aspects of Shape Memory Alloys*. United Kingdom: Elsevier; 1990
- [68] Chentouf SM et al. Microstructural and thermodynamic study of hypoeutectoidal Cu–Al–Ni shape memory alloys. *Journal of Alloys and Compounds*. 2009;**470**(1-2):507-514
- [69] Ratchev P, Van Humbeeck J, Delaey L. On the formation of 2H stacking sequence in 18R martensite plates in a precipitate containing CuAlNiTiMn alloy. *Acta Metallurgica et Materialia*. 1993;**41**(8):2441-2449

- [70] Recarte V, Hurtado I, Herreros J, N6 ML, San Juan J. Precipitation of the stable phases in Cu-Al-Ni shape memory alloys. *Scripta Materialia*. 1996;**34**:255-260
- [71] Font J et al. Thermal cycling effects in high temperature Cu-Al-Ni-Mn-B shape memory alloys. *Journal of Materials Research*. 1997;**12**(9):2288-2297
- [72] Morris MA. Microstructural influence on ductility and shape memory effect of some modified Cu.Ni.Ai alloys. *Scripta Metallurgica*. 1991;**25**:1409-1414
- [73] Lojen G et al. Microstructure of rapidly solidified Cu-Al-Ni shape memory alloy ribbons. *Journal of Materials Processing Technology*. 2005;**162-163**:220-229
- [74] Fremond M, Miyazaki S. *Shape Memory Alloys*. Wien, New York: Springer-Verlag; 1996
- [75] Prasad K et al. *Metallic biomaterials: Current challenges and opportunities*. *Materials*. 2017;**10**(8):884
- [76] Formentini M, Lenci S. An innovative building envelope (kinetic façade) with shape memory Alloys used as actuators and sensors. *Automation in Construction*. 2018;**85**:220-231
- [77] Otsuka K, Wayman CM. *Shape Memory Materials*. Cambridge: Cambridge University Press; 1998
- [78] Miyazaki KOS, Sakamoto H, Shimizu K. Study of fracture in Cu-Al-Ni shape memory bicrystals. *Transactions of the Japan Institute of Metals*. 1981;**22**:244-252
- [79] Husain SW, Clapp PC. Grain boundary embrittlement in Cu-Al-Ni β phase alloys. *Journal of Materials Science*. 1987;**22**:2351-2356
- [80] Dalvand P et al. Properties of rare earth added Cu-12wt% Al-3wt% Ni-0.6 wt% Ti high temperature shape memory alloy. *Materials Science and Engineering: A*. 2019;**754**:370-381
- [81] Edwards TEJ et al. Slip bands in lamellar TiAl during high cycle fatigue microcompression by correlative total strain mapping, diffraction orientation mapping and transmission electron imaging. *International Journal of Fatigue*. 2019;**124**:520-527
- [82] Lee JS, Wayman CM. Grain refinement of Cu-Zn-Al shape memory alloys. *Metallurgy*. 1986;**19**(4):401-419
- [83] Sure GN, Brown LC. The mechanical properties of grain refined β -Cu-Al-Ni strain-memory alloys. *Metallurgical and Materials Transactions A*. 1984;**15**:1613-1621
- [84] Bhattacharya S, Bhuniya A, Banerjee MK. Influence of minor additions on characteristics of Cu-Al-Ni alloy. *Materials Science and Technology*. 1993;**9**(8):654-658
- [85] Adachi K, Hamada Y, Tagawa Y. Crystal structure of the X-phase in grain-refined Cu-Al-Ni-Ti shape memory alloys. *Scripta Metallurgica*. 1987;**21**(4):453-458
- [86] Kim J et al. Effects on microstructure and tensile properties of a zirconium addition to a Cu-Al-Ni shape memory alloy. *Metallurgical and Materials Transactions A*. 1990;**21**(2):741-744
- [87] Morris MA, Lipe T. Microstructural influence of Mn additions on thermoelastic and pseudoelastic properties of Cu-Al-Ni alloys. *Acta Metallurgica et Materialia*. 1994;**42**(5):1583-1594
- [88] Gao Y, Zhu M, Lai JKL. Microstructure characterization and effect of thermal cycling and ageing on vanadium-doped Cu-Al-Ni-Mn

high-temperature shape memory alloy. *Journal of Materials Science*. 1998;**33**(14):3579-3584

[89] Oliveira J et al. Microstructure and mechanical properties of gas tungsten arc welded Cu-Al-Mn shape memory alloy rods. *Journal of Materials Processing Technology*. 2019;**217**:93-100

[90] Yang S et al. Excellent superelasticity and fatigue resistance of Cu-Al-Mn-W shape memory single crystal obtained only through annealing polycrystalline cast alloy. *Materials Science and Engineering: A*. 2019;**749**:249-254

[91] Tian J et al. Process optimization, microstructures and mechanical properties of a Cu-based shape memory alloy fabricated by selective laser melting. *Journal of Alloys and Compounds*. 2019;**785**:754-764

[92] Mazzer E, Milhorato F. Effects of aging on a spray-formed Cu-Al-Ni-Mn-Nb high temperature shape memory alloy. *Materials Science and Engineering: A*. 2019;**753**:232-237

[93] Adachi K, Shoji K, Hamada Y. Formation of (X) phases and origin of grain refinement effect in Cu-Al-Ni shape memory Alloys added with Titanium. *ISIJ International*. 1989;**29**(5):378-387

[94] Vajpai SK, Dube RK, Sangal S. Microstructure and properties of Cu-Al-Ni shape memory alloy strips prepared via hot densification rolling of argon atomized powder preforms. *Materials Science and Engineering A*. 2011;**529**(1):378-387

[95] Guniputi BN, Murigendrappa S. Influence of Gd on the microstructure, mechanical and shape memory properties of Cu-Al-Be polycrystalline shape memory alloy. *Materials Science and Engineering: A*. 2018;**737**:245-252

[96] Hussain S, Pandey A, Dasgupta R. Designed polycrystalline ultra-high ductile boron doped Cu-Al-Ni based shape memory alloy. *Materials Letters*. 2019;**240**:157-160

[97] Zhu M et al. Cheminform abstract: Preparation of single crystal CuAlNiBe SMA and its performances. *ChemInform*. 10 2009;**478**(1-2):404-410

[98] MAaSG M. Effect of heat treatment and thermal cycling on transformation temperatures of ductile Cu-Al-Ni-Mn-B alloys. *Scripta Metallurgica et Materiala*. 1992;**26**(11):1663-1668

[99] Roh DW, Kim JW, Cho TJ, Kim YG. Tensile properties and microstructure of microalloyed Cu-Al-Ni-X shape memory alloys. *Materials Science and Engineering: A*. 1991;**136**:17-23

[100] Zubair I, Khan AQ. Fascinating shape memory alloys. *Journal of the Chemical Society of Pakistan*. 2018;**40**(1):1-23

[101] Punburi P et al. Correlation between electron work functions of multiphase Cu-8Mn-8Al and de-alloying corrosion. *Applied Surface Science*. 2018;**439**:1040-1046

[102] XU, H., et al. A study on shape memory performance of single crystal Cu-Al-Ni-Be alloy. *Materials Review*. 2008;**4**:036

[103] Xu HP, Song GF, Mao XM. Influence of Be and Ni to Cu-Al alloy shape memory performance. *Advanced Materials Research*. 2011;**197**:1258-1262

[104] Gomes RM et al. Pseudoelasticity of Cu-13.8Al-Ni Alloys containing V and Nb. *Advances in Science and Technology*. 2008;**59**:101-107

[105] Zhu M et al. Preparation of single crystal CuAlNiBe SMA and its

performances. *Journal of Alloys and Compounds*. 2009;**478**(1):404-410

[106] Hodgson D, Wu MH, Biermann RJ. *Metals Handbook*. Vol. 2. Ohio: ASM International; 1990. p. 897

[107] Gall K et al. Thermomechanics of the shape memory effect in polymers for biomedical applications. *Journal of Biomedical Materials Research Part A*. 2005;**73**(3):339-348

[108] Wen C et al. Mechanical Behaviors and Biomedical Applications of Shape Memory Materials: A Review. *AIMS Materials Science*. 2018;**5**(4):559-590

[109] Sokolowski WM. *Cold Hibernated Elastic Memory Structure: Self-Deployable Technology and Its Applications*. Florida, United States: CRC Press; 2018

[110] Baghani M, Ganjani M, Rezaei M. Numerical analysis of growing the ductile damage in structures reinforced by SMA using continuum damage mechanics approach. *International Journal of Applied Mechanics*. 2018;**10**(07):1850070

[111] Velmurugan C et al. Machining of NiTi-shape memory alloys-a review. *Machining Science and Technology*. 2018;**22**(3):355-401

[112] Leo DJ et al. Vehicular applications of smart material systems. In: *5th Annual International Symposium on Smart Structures and Materials*. California, United States: International Society for Optics and Photonics; 1998

[113] Stoeckel D. Shape memory actuators for automotive applications. *Materials & Design*. 1990;**11**(6):302-307

[114] Rao A, Srinivasa A. A thermodynamic driving force approach for analyzing functional degradation of shape memory alloy components. *Mechanics of Advanced Materials*

and Structures. 2018. p. 1-13. DOI: 10.1080/15376494.2018.1444229

[115] Wilkes KE, Liaw PK. The fatigue behavior of shape-memory alloys. *JOM*. 2000;**52**(10):45-51

[116] Sellitto A, Riccio A. Overview and future advanced engineering Applications for morphing surfaces by shape memory alloy materials. *Materials*. 2019;**12**(5):708

[117] Leal PB, Savi MA. Shape memory alloy-based mechanism for aeronautical application: Theory, optimization and experiment. *Aerospace Science and Technology*. 2018;**76**:155-163

[118] Kaya E, Kaya İ. A review on machining of NiTi shape memory alloys: The process and post process perspective. *The International Journal of Advanced Manufacturing Technology*. 2019;**100**(5-8):2045-2087

[119] Strittmatter J, Hieber MEM, Gümpel P. Intelligent materials in modern production-current trends for thermal shape memory alloys. *Procedia Manufacturing*. 2019;**30**:347-356

[120] Hornbogen E. Review thermo-mechanical fatigue of shape memory alloys. *Journal of Materials Science*. 2004;**39**(2):385-399

[121] Karakoc O et al. Effects of Testing Parameters on the Fatigue Performance NiTiHf High Temperature Shape Memory Alloys. San Diego, California: AIAA Scitech, Forum; 2019. DOI. org/10.2514/6.2019-0416

[122] Gédouin P-A et al. R-phase shape memory alloy helical spring based actuators: Modeling and experiments. *Sensors and Actuators A: Physical*. 2019;**289**:65-76

[123] Widdle RD et al., High stiffness shape memory alloy actuated aerostructure. Google Patents; 2013

[124] Mani R, Lagoudas DC, Rediniotis OK. MEMS-based active skin for turbulent drag reduction. In: Smart Structures and Materials. California, United States: International Society for Optics and Photonics; 2003

[125] Tawfik M, Ro J-J, Mei C. Thermal post-buckling and aeroelastic behaviour of shape memory alloy reinforced plates. *Smart Materials and Structures*. 2002;**11**(2):297

[126] Furuya Y, Shimada H. Shape memory actuators for robotic applications. *Materials & Design*. 1991;**12**(1):21-28

[127] Sreekumar M et al. Critical review of current trends in shape memory alloy actuators for intelligent robots. *Industrial Robot: An International Journal*. 2007;**34**(4):285-294

[128] Wu MH, Schetky L. Industrial applications for shape memory alloys. In: *Proceedings of the International Conference on Shape Memory and Superelastic Technologies*; Pacific Grove, California. 2000

[129] Russell SM. SMST-2000: *Proceedings of the International Conference on Shape Memory and Superelastic Technologies*. Oxfordshire, United Kingdom: SMST, The International Organization on Shape Memory and Superelastic Technology; 2001